

Strain-Dependent Viral Dynamics and Virus-Cell Interactions in a Novel *In Vitro* System Supporting the Life Cycle of Blood-Borne Hepatitis C Virus

Hussein Hassan Aly,^{1,2} Yue Qi,³ Kimie Atsuzawa,⁴ Nobuteru Usuda,⁴ Yasutsugu Takada,⁵ Masashi Mizokami,⁶ Kunitada Shimotohno,⁷ and Makoto Hijikata^{1,3}

We developed an *in vitro* system that can be used for the study of the life cycle of a wide variety of blood-borne hepatitis C viruses (HCV) from various patients using a three-dimensional hollow fiber culture system and an immortalized primary human hepatocyte (HuS-E/2) cell line. Unlike the conventional two-dimensional culture, this system not only enhanced the infectivity of blood-borne HCV but also supported its long-term proliferation and the production of infectious virus particles. Both sucrose gradient fractionation and electron microscopy examination showed that the produced virus-like particles are within a similar fraction and size range to those previously reported. Infection with different HCV strains showed strain-dependent different patterns of HCV proliferation and particle production. Fluctuation of virus proliferation and particle production was found during prolonged culture and was found to be associated with change in the major replicating virus strain. Induction of cellular apoptosis was only found when strains of HCV-2a genotype were used for infection. Interferon-alpha stimulation also varied among different strains of HCV-1b genotypes tested in this study. **Conclusion:** These results suggest that this *in vitro* infection system can reproduce strain-dependent events reflecting viral dynamics and virus-cell interactions at the early phase of blood-borne HCV infection, and that this system can allow the development of new anti-HCV strategies specific to various HCV strains. (HEPATOLOGY 2009;50:689-696.)

Hepatitis C virus (HCV) is a serious problem worldwide, with 3% of the world's population chronically infected.¹ Chronic infection with HCV may lead to high rates of liver cirrhosis and hepatocellular carcinoma.² Because the HCV standard therapy is still insufficient for treating many patients,³ the develop-

ment of more effective and less toxic anti-HCV agents is desired. The virological studies required to reach this goal need reproducible and efficient HCV proliferation in cell culture. An *in vitro* infection system using recombinant HCV-JFH1 was developed. In this system, HuH7 cells transfected with *in vitro*-synthesized JFH1-RNA were

Abbreviations: 2D, two-dimensional; 2D-HuS-E/2, HuS-E/2 cells cultured in two-dimensional condition; 3D, three-dimensional; 3D/HF, 3D hollow fibers; 3D-HuS-E/2, HuS-E/2 cells cultured in three-dimensional condition in the hollow fibers; HCV, hepatitis C virus; IFN- α , interferon alpha; LDH, lactate dehydrogenase; p.i., postinfection; RFB, radial-flow bioreactor; RT-PCR, reverse transcription polymerase chain reaction.

From the ¹Laboratory of Human Tumor Viruses, Institute for Virus Research, Kyoto University, Kyoto, Japan; ²Hepatology Department, National Hepatology and Tropical Medicine Research Institute, Cairo, Egypt; ³Laboratory of Viral Oncology, Graduate School of Biostudies, Kyoto University, Kyoto, Japan; ⁴Department of Anatomy, Fujita Health University School of Medicine, Toyoake, Japan; ⁵Department of Surgery, Division of Hepato-Pancreato-Biliary and Transplant Surgery, Graduate School of Medicine, Kyoto University, Kyoto, Japan; ⁶Research Center for Hepatitis and Immunology, International Medical Center of Japan Koinodai Hospital, Ichikawa, Japan; ⁷Center for Human Metabolomic Systems Biology, Keio University, Tokyo, Japan.

Received November 12, 2008; accepted April 9, 2009.

Supported by grants-in-aid from the Ministry of Health, Labor and Welfare of Japan; by grants-in-aid from Japan Health Sciences Foundation; and by grants-in-aid for scientific research from Ministry of Education, Sports, Culture, and Technology of Japan.

Address reprint requests to: Kunitada Shimotohno, Ph.D., Center for Human Metabolomic Systems Biology, Keio University, 35, Shinano-machi, Shinjuku-ku, Tokyo, 160-8582, Japan. E-mail: shimkuni@z8.keio.jp; fax: 81-3-5363-3592; or Makoto Hijikata, Ph.D., Laboratory of Human Tumor Viruses, Institute for Virus Research, Kyoto University, 53, Kawabara-cho, Shogoin, Sakyo-ku, Kyoto, 606-8507, Japan. E-mail: mhijikat@virus.kyoto-u.ac.jp; fax: 81-75-751-3998.

Copyright © 2009 by the American Association for the Study of Liver Diseases.

Published online in Wiley InterScience (www.interscience.wiley.com).

DOI 10.1002/hep.23034

Potential conflict of interest: Nothing to report.

Additional Supporting Information may be found in the online version of this article.

shown to secrete infectious viral particles.⁴ This system, however, requires the combination of HuH-7-derived cell lines and JFH1-based constructs, limiting its usefulness for studying other HCV strains. Because HuH-7 cells cannot support the complete life cycle of blood-borne HCV (bbHCV) derived from clinical samples,⁵ this system is insufficient for studying all the events related to bbHCV infection.

Many researchers have attempted to develop an *in vitro* system for bbHCV.⁶⁻⁸ These current systems, however, are still insufficient due to their low efficiency for infectivity and replication of bbHCV. Working toward this same goal, we recently established immortalized primary human hepatocyte cell lines by transducing them with E6 and E7 genes from the human papilloma virus 18.^{5,9} As expected, we observed improved infection and replication of bbHCV especially in one of these cell lines (HuS-E/2 cells) that showed a similar expression profile to that of human primary hepatocytes, but this strategy did not improve production of infectious particles.

Recently, a hybrid artificial liver support system was developed using animal hepatocytes cultured in a three-dimensional hollow fiber (3D/HF) system. This bioartificial liver showed several characteristic features of liver tissue for more than 4 months.¹⁰⁻¹² By growing our HuS-E/2 cells in a similar 3D culture⁵ the gene expression profile was improved to more closely match that of human primary hepatocytes. Because the 3D cell culture condition more closely reproduces the *in vivo* environment of hepatocytes,¹³ culturing these cells in this manner may support the entire HCV life cycle.

In this study we utilized this small 3D culture system and showed it to be ideal for culturing HuS-E/2 cells for the study of bbHCV infection. Using this system we are now able to study the variable patterns of the life cycle of different bbHCV strains as well as HCV-related cellular events.

Materials and Methods

Cell Culture. HuS-E/2 cells were cultured as previously described.⁵ For the 3D/HF system, HuS-E/2 suspension was injected into the lumen of HF (Toyobo, Osaka, Japan) made from cellulose acetate and containing pores for nutrients and waste exchange (Supporting Fig. 1). The bundles were centrifuged to induce organoid formation. The cells in the fibers were cultured in 12-well plates (two capillary bundles per well) with gentle rotation using serum-free medium (Toyobo) in a CO₂ incubator at 37°C. The number of cells was adjusted to 3 × 10⁵ cells per two-capillary bundle at the start of each experiment.

RNA Experiments. Total RNA was extracted from two-dimensional (2D) cultured cells, patient sera, or from 100 times concentrated culture medium as previously described.^{4,5} For cells cultured in the 3D/HF, sterile scissors were used to cut each fiber into small pieces (1 mm² each), which were then solubilized in Sepasol RNA-1 (Nacalai Tesque, Kyoto, Japan). RNA was then extracted according to the manufacturer's protocol. Real-time reverse transcription polymerase chain reaction (RT-PCR) was performed as described.⁵

HCV Infection. HCV infection experiments were carried out using sera from HCV patients. The amount of each inoculum was adjusted so as to add similar amount of HCV-RNA to the medium of the cells. After 24 hours, the cells were washed three times with phosphate-buffered saline (PBS) and cultured for the designated times. To assess the passage of infectivity, 12 mL of culture medium from the primary infected cells was collected, concentrated 100 times by filtration through Amicon Ultra-15, Ultracel-10K filters (Millipore, Carrigtwohill, Cork, Ireland), and 40 μL concentrated medium/well was used to infect naïve HuS-E/2 cells. All experiments were done with approval of the Ethical Committee of Kyoto University. Informed consent from patients was required for this approval.

Cloning and Sequencing. To amplify the complementary DNA (cDNA) fragment corresponding to hypervariable region 1 (HVR-1),¹⁴ a nested RT-PCR was performed using Superscript III (Invitrogen, Carlsbad, CA) and PrimeSTAR HS DNA Polymerase (Takara, Tokyo, Japan). Reaction conditions were adjusted according to the manufacturer's protocol. Primers used were previously described¹⁵ and are shown in Supporting Table 1. PCR products were then purified and cloned using the Zero Blunt TOPO PCR Cloning Kit (Invitrogen). Ten recombinant clones were randomly isolated for each PCR product and sequenced as described.¹⁶

Quantitative Detection of HCV Core and Interferon alpha (IFN-α) Protein by Enzyme-Linked Immunosorbent Assay (ELISA). The culture medium of infected cells was collected and concentrated 100 times as previously mentioned for the detection of HCV-core, or used directly for detection of IFN-α. HCV core protein was quantified using the Trak-C Core ELISA (Ortho Clinical Diagnostics, Neckargemünd, Germany). IFN-α was quantified using the Human IFN-A ELISA kit (PBL Biomedical Laboratories, Piscataway, NJ). Light absorbance was then measured using a Wallac 1420 multilabel counter (PerkinElmer Life Science, Waltham, MA).

Cytotoxicity Assay. Culture medium was collected from HCV-infected cells and used for measuring lactate dehydrogenase (LDH) levels using an LDH cytotoxicity

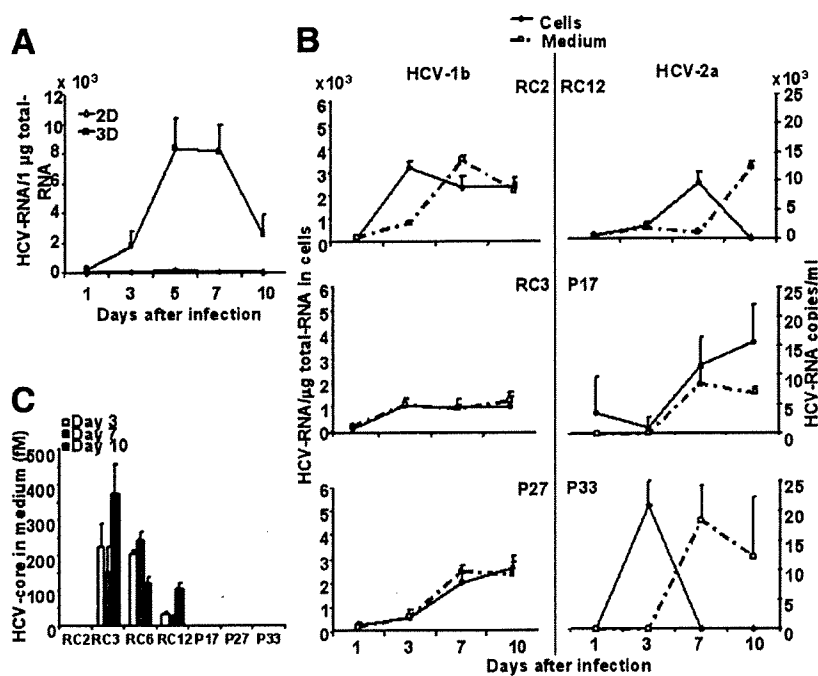


Fig. 1. Infection and proliferation of bbHCV in 3D-HuS-E/2 cells. (A) The quantity of HCV genomic RNA in 1 μ g total RNA of 2D- or 3D-HuS-E/2 cells infected with HCV-RC6 was determined at each timepoint after infection by real-time RT-PCR analysis. (B) 3D-HuS-E/2 cells were infected with HCV-1b-containing sera: RC2, RC3, and P27; or HCV-2a-containing sera: 4: RC12, P17, P33. The quantity of HCV genomic RNA in the infected cells was determined as in (A). The culture medium from the last 2 days at each timepoint was collected, concentrated, and the amount of HCV-RNA (B) or HCV-core (C) was measured. Data represent the mean \pm standard deviation (SD) of three independent experiments.

detection kit (Takara Biomedicals). Light absorbance was then measured as described above.

Sucrose Density Gradient. The culture medium of the infected cells was collected, concentrated 500 times, and loaded onto a 20%-50% (wt/vol) sucrose gradient containing 50 mM PBS, 100 mM NaCl, and 1 mM EDTA, followed by centrifugation at 100,000g for 16 hours at 4°C in a SW41Ti rotor (Beckman, Fullerton, CA). The gradient was fractionated into 31 fractions that were used for HCV-RNA and core detection and HCV infection into naïve cells as described above.

Electron Microscopy. The 1.12 g/mL fraction obtained by the sucrose density gradient showed the secondary infection activity as analyzed by transmission electron microscopy. The fraction was ultracentrifuged and the almost all supernatant was removed. The residual 10 μ L of the solution was directly applied to a formvar-carbon grid for negative staining with 1% uranyl acetate solution and observed with an electron microscope (JEOL1010, JEOL, Tokyo, Japan).

Results

HuS-E/2 Cells Cultured in 3D/HF System Are Highly Permissive for Infection and Proliferation of bbHCV. We compared the ability of HuS-E/2 cells cultured in the 3D/HF system (3D-HuS-E/2 cells) to those cultured as a monolayer (2D-HuS-E/2 cells) to reproduce infection by HCV genotype 1b (HCV-RC6), derived from patient serum (RC6). The HCV-RC6 RNA levels in

the 3D-HuS-E/2 cells were significantly higher at all timepoints (Fig. 1A), showing that the 3D/HF system greatly improves the proliferation of bbHCV in HuS-E/2 cells. We observed that both the early stages of infection and the continuous replication of HCV-RC6 in HuS-E/2 cells was improved by 3D/HF culture when the culture conditions were changed after the infection from 3D/HF to 2D and vice versa (Supporting Fig. 2).

As reported,¹⁷ blocking CD81, an HCV-supposed entry receptor, during infection significantly impaired HCV proliferation into 3D-HuS-E/2 cells (Supporting Fig. 3), suggesting that CD81 is essential for HCV infectivity in 3D-HuS-E/2 cells. Although the expression level of CD81 mRNA in 3D-HuS-E/2 cells was observed, no significant change from 2D-HuS-E/2 cells was found (data not shown), indicating that the quantity of CD81, at least, is not responsible for the improvement.

We then examined whether this system can be used for proliferation of six different bbHCV samples, three of which are HCV-1b (HCV-RC2, HCV-RC3, and HCV-P27) and three HCV-2a genotypes (HCV-RC12, HCV-P17, and HCV-P33) (Fig. 1B). Proliferation of HCV-RNA in the cells was seen in all six cases, suggesting that this system can be widely used for analysis of infection and proliferation of bbHCV strains. HCV-RNA and HCV-core were also detected in the culture medium (Fig. 1B). Different HCV strains showed variable patterns of proliferation and HCV-core secretion into the medium. Although HCV-core was detected from day 3 onward when

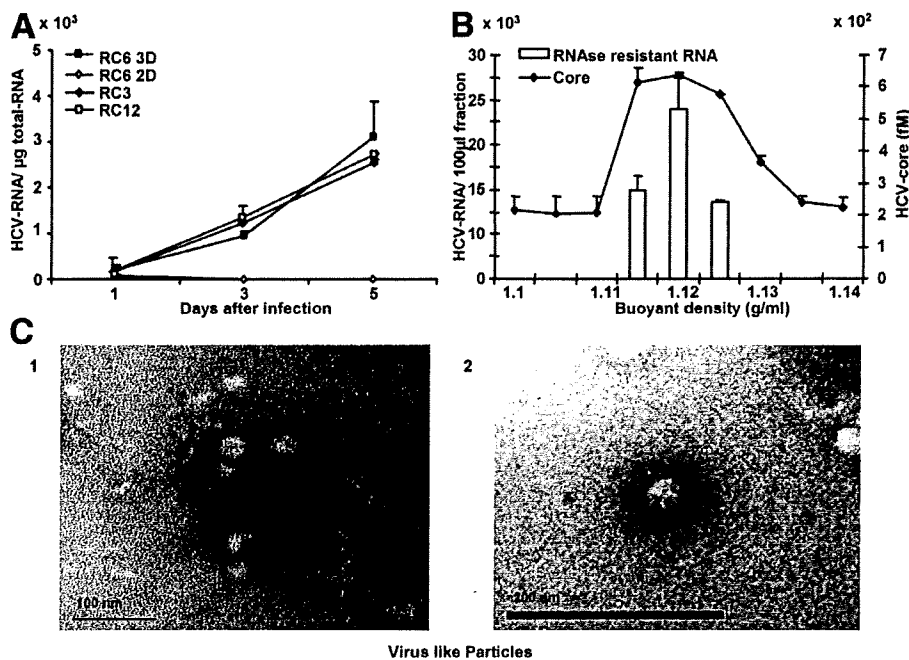


Fig. 2. Production of infectious virus-like particles from 3D-HuS-E/2 cells infected with different HCV strains. (A) The culture medium of 3D-HuS-E/2 cells infected with HCV-RC3 or HCV-RC6 was collected from days 5 to 7 p.i. and for HCV-RC12 from days 23 to 25 p.i. The culture medium of 2D-HuS-E/2 cells infected with HCV-RC6 was also collected from days 5 to 7 p.i., and used to treat naïve 3D-HuS-E/2 cells. The quantity of HCV genomic RNA in 1 μ g of total cellular RNA was determined as in Fig. 1. (B) The concentrated culture medium of 3D-HuS-E/2 cells infected with HCV-RC3 was collected from days 5 to 7 p.i., and fractionated by ultracentrifugation with a 20%-50% sucrose density gradient. HCV-core protein and the RNase A-resistant HCV-RNA in the different fractions were quantitatively analyzed using an HCV-core ELISA kit and real-time RT-PCR, respectively. Data represent the mean \pm SD of three independent experiments. (C) Photomicrograph showing negatively stained virus-like particles from the culture medium of HCV-RC3-infected 3D-HuS-E/2 cells (arrowheads, panels 1 and 2). The arrows indicate the spike-like structures found on the surface of the virus-like particles (panel 2).

RC3, RC6, and RC12 were used for infection, it was undetectable when RC2, P17, P27, and P33 sera were used, similar to 2D-HuS-E/2 cells infected with HCV-RC6 (Fig. 1C).

Production of Infectious Particles from 3D-HuS-E/2 Cells Infected with bbHCV. The culture media from 2D or 3D-HuS-E/2 cells infected with RC6 serum (Fig. 1A) were collected from days 5 to 7 postinfection (p.i.), concentrated, and inoculated into naïve 3D-HuS-E/2 cell culture media. HCV-RNA's proliferation in the infected cells was only detected when using the culture medium from 3D-HuS-E/2 cells and not 2D-HuS-E/2 cells (Fig. 2A). Media collected from HCV-RC3 at days 5 to 7 and from HCV-RC12 from days 23 to 25 p.i. were also able to infect naïve cells (Fig. 2A). These data suggested the production and secretion of infectious virus-like particles. To investigate this further, biophysical analysis was performed. The culture medium of HCV-RC3 infected 3D-HuS-E/2 cells at day 7 p.i. was fractionated using a sucrose density gradient after RNase A treatment. HCV core was detected in the 1.11 to 1.14 g/mL fractions; similarly, the nuclease-resistant HCV RNA peaked in the 1.12 g/mL fraction (Fig. 2B). Fur-

thermore, only the 1.12 g/mL fraction was able to infect naïve cells as examined above (data not shown). This fraction was pelleted by ultracentrifugation and examined by electron microscopy with negative staining. We observed 33-nm to 45-nm diameter spherical particles (Fig. 2C, panel 1) with spike-like structures from 7-9 nm in length on the surface (Fig. 2C, panel 2), consistent with HCV morphology reported previously in HCV patients.¹⁸ These were detected in the sample collected from HCV-RC3-treated but not mock-treated 3D-HuS-E/2 cells. These data suggest that production of infectious virus-like particles occurs in 3D-HuS-E/2 cells infected with some bbHCV strains. It is therefore likely that 3D-HuS-E/2 cells can be used to reproduce nearly all steps in the HCV life cycle.

Prolonged Culture of HCV-Infected Cells in the 3D Hollow Fiber System. For HCV-RC6-infected cells (Fig. 3A), the amount of HCV-RNA in the cells fluctuated during the 30-day culture period. The levels of both HCV-RNA and HCV-core in the medium showed a similar pattern of fluctuations that peaked on days 5 and 20 p.i. Unlike RC6, the pattern of HCV-RNA levels in the medium of RC12-infected cells showed a negative

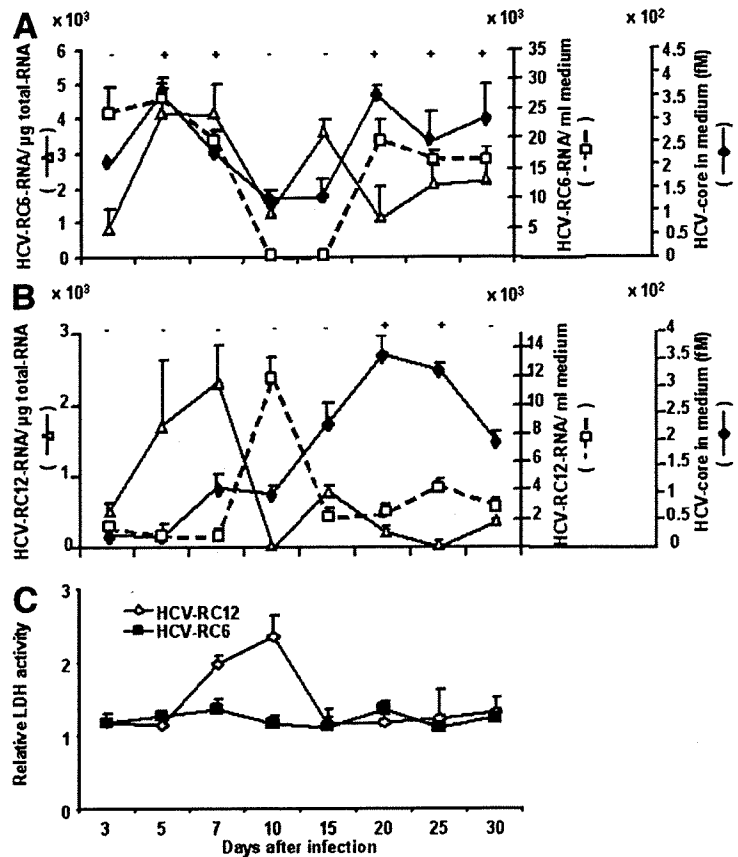


Fig. 3. Prolonged culture of HCV-infected cells in the 3D/HF system. After infection with HCV-RC6 (A) and HCV-RC12 (B), 3D-HuS-E/2 cells were cultured for 30 days with a medium change every 2 days. The HCV-RNA in the cells and medium as well as the HCV-core in the medium were quantitatively analyzed at the designated timepoints as in Fig. 1. Culture media were also used to treat naïve 3D-HuS-E/2 cells to examine the secondary infection as in Fig. 2. (+) and (-) indicate detection or no detection of secondary infection. (C) Culture media of HCV-RC6 and HCV-RC12 infected cells collected at each timepoint were used for the detection of LDH levels released from dead cells. LDH levels were normalized to uninfected cells cultured for the same time. Data represent the mean ± SD of three independent experiments.

correlation with that detected in the cells. This was clearly seen on day 10 p.i., when a sharp increase and decrease of HCV-RNA in the medium and the cells, respectively, was observed (Fig. 3B). Similarly, the amount of HCV-core detected in the medium throughout the culture was not correlated with RNA levels in the medium. Instead, core levels were very low in the first 10 days, at which time levels increased, reaching a peak on day 20 p.i. (Fig. 3B). Culture media from cells infected with HCV-RC6 from days 5 to 7 and 20 to 30 p.i. (Fig. 3A) and that from HCV-RC12 from days 20 to 25 p.i. showed passage of infectivity (Fig. 3B). All culture media showing infectivity appeared to have a high amount of HCV-core protein.

Clonal Changes in HCV During Prolonged Culture. In order to perform a populational analysis to understand the fluctuating pattern seen during HCV proliferation, two sera with limited HCV variants, HCV-RC6 (two major strains) and -RC12 (single major strain) from immunosuppressed liver transplantation patients with recurrent HCV were used in the previous prolonged infection experiment. The variants' composition was analyzed by single-strand confirmation polymorphism analysis for HCV-HVR1 (Supporting Fig. 4). RC6 serum (Fig. 4A) showed two different major sequences, HCV-

RC6-1 and -2 strains, which constituted 60% and 40%, respectively, and shared 85% homology. In cells infected with HCV-RC6 the nucleotide sequence of HVR1 on day 5 showed 97% homology to HCV-RC6-1, and on day 20 p.i. it showed 97% homology to HCV-RC6-2. These data suggest selection of the dominant HCV strain in the cells over time. For RC12 (Fig. 4B), the nucleotide sequence on day 5 p.i. had only one nucleotide difference from that of the HCV from the original serum. The sequence from day 20 p.i. was four nucleotides different from that from the serum, and five different from the cells on day 5 p.i. These data indicated that each peak of HCV-RNA that appeared in the cells infected with RC12 serum included primarily a single HCV strain with a slightly different genomic sequence. This suggests that the periodic appearance of HCV-RNA peaks in the cells infected with a particular HCV strain is a result of selection and/or mutation of HCV strains during the prolonged culture period.

Cellular Response Induced by bbHCV Infection. At day 10 p.i., HCV-RNA levels in the culture medium rose and RNA levels in 3D-HuS-E/2 cells infected with HCV-RC12 dropped (Figs. 1B, 3B). To determine if this was caused by a cytotoxic effect of HCV infection, LDH levels were measured in the culture medium of HCV-RC6- and

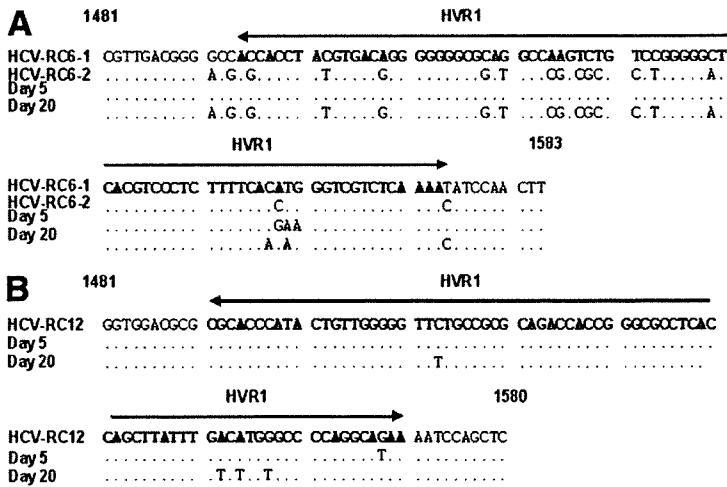


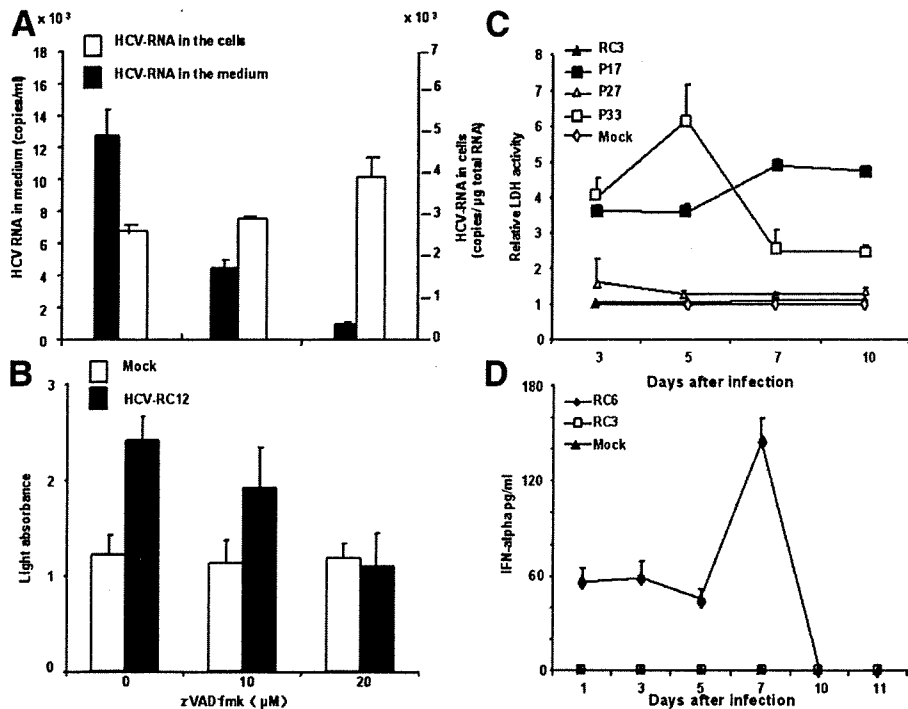
Fig. 4. Comparison of HCV-HVR1 sequences in the serum used for infection and the HCV replicating in the cells on days 5 and 20 after infection of HCV-RC6 (A) or HCV-RC12 (B). Nucleotide numbering was based on HCV-J1 sequence (GenBank Access. No. D10749). Three additional nucleotides were found at the 5'-terminal end of the E2 regions of all RC6 sequences. The major sequence present in the serum used for infection is shown in the upper row in each panel. Dots represent the identical nucleotides.

HCV-RC12-infected 3D-HuS-E/2 cells. LDH activity showed a strong correlation with HCV-RNA levels in the medium on day 10 p.i. in HCV-RC12-infected cells (Fig. 3B), suggesting a cytotoxic effect of HCV-RC12 that was not observed in the case of HCV-RC6 (Fig. 3A,C). To determine if this HCV infection-mediated cytotoxicity is due to apoptosis, as with other viruses belonging to the Flaviviridae family,¹⁹ the involvement of caspase was examined using the caspase inhibitor z-VAD-fmk. A significant dose-dependent reduction in HCV-RNA levels in the medium and LDH activity (Fig. 5A,B) was found, whereas no significant effect was observed on the viability

of noninfected cells (Fig. 5B) or intracellular HCV-RNA levels (Fig. 5A). This suggested that the cytotoxic effect of HCV infection is mediated by apoptosis. It is noteworthy that HCV-induced cytopathicity was also found when HCV-P17 and HCV-P33 samples were used for infection (both are HCV-2a genotype) and was not reproduced in any of the HCV-1b genotype samples used in this work (Fig. 5C).

After infection with HCV-RC6, no cytotoxicity was detected that might have inhibited HCV-RC6-1 proliferation in the cells. However, HCV-RC6-2 RNA replaced HCV-RC6-1 RNA during prolonged culture. To assess a

Fig. 5. Cellular response of 3D-HuS-E/2 cells infected with bbHCV. 3D-HuS-E/2 cells infected with HCV-RC12 and mock-treated cells were cultured for 10 days in the presence of z-VAD-fmk (0, 10, and 20 μ M). (A) HCV-RNA in the cells and medium on day 10 was measured as in Fig. 1. (B) LDH levels in the medium on day 10 after infection with HCV-RC12 was measured as in Fig. 3. (C) Culture media of HCV-RC3, HCV-P17, HCV-P27, HCV-P33, and mock-infected cells collected at designated points were used for the detection of LDH levels. (D) IFN- α levels in the culture media of HCV-RC6, HCV-RC3, and mock-infected cells collected at each designated timepoint were measured by ELISA. Data represent the mean \pm SD of three independent experiments.



possible role of the innate-immune response in this phenomenon, the production of IFN- α in the medium was measured during the first 11 days p.i. IFN- α production was detected as early as day 1 p.i., reached a peak at day 7 p.i., and was then rapidly lost (Fig. 5D). These data suggest that HCV-RC6-1 infection induced the innate-immune response of the cells, possibly leading to suppression of its proliferation. In contrast to HCV-RC6-1, HCV-RC3 did not show any stimulation of IFN- α production upon infection in the first 10 days, showing a possible strain-dependent evasion from the host defense within the same genotype.

Discussion

In this study we report the development of a novel system that reproduces bbHCV infection, proliferation, and production of infectious virus. The most recent models used in the study of the life cycle of HCV infection are based on subclones of HuH-7 cells infected with JFH1 recombinant virus or its derivatives.⁴ HuH-7 cells and its subclones, however, do not support the entire life cycle of the bbHCVs present in patients' blood.⁵ Moreover, HCV has considerable diversity and variability. It is generally classified into six major genotypes and more than 100 subtypes.²⁰ This huge pool of natural HCV variants causes a wide variety of diseases, including chronic hepatitis, cirrhosis, and hepatocellular carcinoma.²¹ JFH1, however, is a single isolate of HCV genotype 2a that was originally derived from a patient with rare fulminant hepatitis.⁴ We suggest that our newly established system has an important advantage because it supports the entire life cycle of a variety of HCV strains and genotypes.

Due to the lack of some *in vivo* factors, including host immune response, *in vitro* systems may not completely reproduce the *in vivo* situation. However, *in vitro* experimental systems seem to be important to simplify particular events from the complex situation *in vivo*. From that standpoint, our cell culture system is likely reproducing the early event of HCV infection in the absence of host-immune responses and supporting whole life cycle of the blood-borne HCV. Several *in vitro* hepatocyte culture systems have been reported to be useful for studying the infection and replication of bbHCV.^{5-8,22} Only the radial-flow bioreactor (RFB) 3D culture system demonstrated production of infectious viruses.²² In our studies we observed not only the enhancement of HCV replication, but also the production of infectious HCV particles in the medium using the 3D/HF system. These data suggest that some structure of the cell mass formed by the 3D culture system, most likely the polar character, is essential for the life cycle of bbHCV. The RFB system is composed of a dedicated device containing 1×10^9 FLC4 cells with a

culture area of 2.7 m².²² It can only be used to study HCV particle production in the medium and not the cellular events that accompany the HCV life cycle. In contrast, because cells grown in our 3D/HF system are cultured in 12-well plates at a density of 3×10^5 /fiber, it is much simpler to study both viral and cellular events.

The production of infectious particles was not detected with infection by different HCV strains, despite detecting equivalent levels of HCV-RNA in the cells (Fig. 1B,C). Delayed production of infectious particles was also observed in cells infected with HCV-RC12 after prolonged culture. A similar delay was also observed in the RFB system.²² Considering the relative stability of HuS-E/2 cells⁵ and the relatively high frequency of the change in HCV population in the cells,¹⁶ it is likely that mutation of the HCV genome and/or selection of clones during prolonged culture improved the productivity of infectious particles. A marked improvement of infectious particle production by substitution of the structural proteins of the genome was also reported in the recombinant HCV production system.²³ The lack of production of infectious particles soon after infection may serve to avoid an early strong response from the host immune system, and demonstrates a novel mechanism of latent infection by HCV. Although they may not be associated with plasma components as those present *in vivo*, HCV virus-like particles produced by this system showed a close resemblance to those isolated from infected HCV patients because they showed the same size¹⁸ and were within the fraction range.²⁴ They may help in the study of viral and cellular factors required for particle production and the possible receptors utilized for infection with different HCV strains.

Fluctuation in HCV proliferation was observed during the prolonged culture of 3D-HuS-E/2 cells infected with bbHCV (Fig. 3A,B), consistent with previous reports in other culture systems.^{6,22} This fluctuation was associated with a change in viral quasispecies, suggesting that an HCV strain having a growth advantage proliferates selectively and dominantly in these culture conditions. Because the progressive emergence of each dominant strain was only temporary, it is highly likely that the infection and proliferation of such an HCV strain is suppressed by cellular mechanism(s). Our results suggest that there are actually two cellular mechanisms functioning to do this. The first is the involvement of the innate immune system, as evidenced by the secretion of IFN- α during the first week of infection (Fig. 5D). This is the first report of secretion of IFN- α from cultured cells infected with bbHCV. Although recent reports suggest that stimulation of the IFN pathway by HCV infection could be impaired by HCV NS3-4a proteinase-mediated cleavage of IPS-

1,²⁵ our results suggest that not all bbHCVs possess a host cell suppressive function. The second mechanism is HCV-induced cell death (Fig. 3C). Almost all the studies reporting HCV-induced apoptosis used hepatocellular carcinoma cell lines.^{26,27} Because it has been established that the inability to undergo apoptosis is essential for the development of cancer,²⁸⁻³⁰ our use of immortalized, non-cancerous HuS-E/2 hepatocytes may make it possible to reproduce the physiological response of the cells to bbHCV infection more closely. Although HCV-induced apoptosis was not found when HCV-1b was used for infection, it was found in all cases where HCV-2a was used, suggesting a higher cytopathic tendency of the HCV-2a genotype. HCV proliferation was continuously found even after the suppression of the first peak of RNA production during prolonged culture. How HCV survives under those conditions is still unknown. Further studies to clarify the molecular mechanisms involving the HCV-cell interaction can be done using this novel 3D culture system that reproduces the infection of a variety of bbHCVs.

In conclusion, we have established a new *in vitro* culture system that can support the entire life cycle of a variety of HCV isolates and genotypes. Although this *in vitro* model system may not completely reproduce the *in vivo* situation, we believe it is the first *in vitro* system showing HCV strain-dependent virus/cell interaction including induction of cellular apoptosis and/or evasion from cellular innate immune response, which may make it a good tool for analysis of virus/host interaction together with the development of new anti-HCV strategies for the different bbHCV strains.

Acknowledgment: We thank T. Yamaguchi for providing hollow fibers and culture medium.

References

- Wasley A, Alter MJ. Epidemiology of hepatitis C: geographic differences and temporal trends. *Semin Liver Dis* 2000;20:1-16.
- Younossi Z, Kallman J, Kincaid J. The effects of HCV infection and management on health-related quality of life. *HEPATOLOGY* 2007;45:806-816.
- Fried MW, Shiffman ML, Reddy KR, Smith C, Marinos G, Goncalves FL Jr, et al. Peginterferon alfa-2a plus ribavirin for chronic hepatitis C virus infection. *N Engl J Med* 2002;347:975-982.
- Wakita T, Pietschmann T, Kato T, Date T, Miyamoto M, Zhao Z, et al. Production of infectious hepatitis C virus in tissue culture from a cloned viral genome. *Nat Med* 2005;11:791-796.
- Aly HH, Watashi K, Hijikata M, Kaneko H, Takada Y, Egawa H, et al. Serum-derived hepatitis C virus infectivity in interferon regulatory factor-7-suppressed human primary hepatocytes. *J Hepatol* 2007;46:26-36.
- Ikeda M, Sugiyama K, Mizutani T, Tanaka T, Tanaka K, Sekihara H, et al. Human hepatocyte clonal cell lines that support persistent replication of hepatitis C virus. *Virus Res* 1998;56:157-167.
- Chong TW, Smith RL, Hughes MG, Camden J, Rudy CK, Evans HL, et al. Primary human hepatocytes in spheroid formation to study hepatitis C infection. *J Surg Res* 2006;130:52-57.
- Molina S, Castet V, Pichard-Garcia L, Wychowski C, Meurs E, Pascussi JM, et al. Serum-derived hepatitis C virus infection of primary human hepatocytes is tetraspanin CD81 dependent. *J Virol* 2008;82:569-574.
- El-Farrash MA, Aly HH, Watashi K, Hijikata M, Egawa H, Shimotohno K. In vitro infection of immortalized primary hepatocytes by HCV genotype 4a and inhibition of virus replication by cyclosporin. *Microbiol Immunol* 2007;51:127-133.
- Mizumoto H, Ishihara K, Nakazawa K, Ijima H, Funatsu K, Kajiwara T. A new culture technique for hepatocyte organoid formation and long-term maintenance of liver-specific functions. *Tissue Eng Part C Methods* 2008;14:167-175.
- Funatsu K, Ijima H, Nakazawa K, Yamashita Y, Shimada M, Sugimachi K. Hybrid artificial liver using hepatocyte organoid culture. *Artif Organs* 2001;25:194-200.
- Mizumoto H, Aoki K, Nakazawa K, Ijima H, Funatsu K, Kajiwara T. Hepatic differentiation of embryonic stem cells in HF/organoid culture. *Transplant Proc* 2008;40:611-613.
- Andrei G. Three-dimensional culture models for human viral diseases and antiviral drug development. *Antiviral Res* 2006;71:96-107.
- Hijikata M, Kato N, Ootsuyama Y, Nakagawa M, Ohkoshi S, Shimotohno K. Hypervariable regions in the putative glycoprotein of hepatitis C virus. *Biochem Biophys Res Commun* 1991;175:220-228.
- Boulestin A, Sandres-Saune K, Payen JL, Alric L, Dubois M, Pasquier C, et al. Genetic heterogeneity of the envelope 2 gene and eradication of hepatitis C virus after a second course of interferon-alpha. *J Med Virol* 2002;68:221-228.
- Murakami K, Inoue Y, Hmwe SS, Omata K, Hongo T, Ishii K, et al. Dynamic behavior of hepatitis C virus quasispecies in a long-term culture of the three-dimensional radial-flow bioreactor system. *J Virol Methods* 2008;148:174-181.
- Meuleman P, Hesselgesser J, Paulson M, Vanvolleghem T, Desombere I, Reiser H, et al. Anti-CD81 antibodies can prevent a hepatitis C virus infection in vivo. *HEPATOLOGY* 2008;48:1761-1768.
- Kaito M, Watanabe S, Tsukiyama-Kohara K, Yamaguchi K, Kobayashi Y, Konishi M, et al. Hepatitis C virus particle detected by immunoelectron microscopic study. *J Gen Virol* 1994;75:1755-1760.
- Roulston A, Marcellus RC, Branton PE. Viruses and apoptosis. *Annu Rev Microbiol* 1999;53:577-628.
- Forns X, Bukh J. The molecular biology of hepatitis C virus. Genotypes and quasispecies. *Clin Liver Dis* 1999;3:693-716, vii.
- Dickson RC. Clinical manifestations of hepatitis C. *Clin Liver Dis* 1997;1:569-585.
- Aizaki H, Nagamori S, Matsuda M, Kawakami H, Hashimoto O, Ishiko H, et al. Production and release of infectious hepatitis C virus from human liver cell cultures in the three-dimensional radial-flow bioreactor. *Virology* 2003;314:16-25.
- Mateu G, Donis RO, Wakita T, Bukh J, Grakoui A. Intragenotypic JFH1 based recombinant hepatitis C virus produces high levels of infectious particles but causes increased cell death. *Virology* 2008;376:397-407.
- Li X, Jeffers LJ, Shao L, Reddy KR, de Medina M, Scheffel J, et al. Identification of hepatitis C virus by immunoelectron microscopy. *J Viral Hepat* 1995;2:227-234.
- Gale M Jr, Foy EM. Evasion of intracellular host defence by hepatitis C virus. *Nature* 2005;436:939-945.
- Fischer R, Baumert T, Blum HE. Hepatitis C virus infection and apoptosis. *World J Gastroenterol* 2007;13:4865-4872.
- Aoki H, Hayashi J, Moriyama M, Arakawa Y, Hino O. Hepatitis C virus core protein interacts with 14-3-3 protein and activates the kinase Raf-1. *J Virol* 2000;74:1736-1741.
- Ladu S, Calvisi DF, Conner EA, Farina M, Factor VM, Thorgeirsson SS. E2F1 inhibits c-Myc-driven apoptosis via PIK3CA/Akt/mTOR and COX-2 in a mouse model of human liver cancer. *Gastroenterology* 2008;135:1322-1332.
- Lowe SW, Lin AW. Apoptosis in cancer. *Carcinogenesis* 2000;21:485-495.
- Schulze-Bergkamen H, Krammer PH. Apoptosis in cancer—implications for therapy. *Semin Oncol* 2004;31:90-119.



3D cultured immortalized human hepatocytes useful to develop drugs for blood-borne HCV

Hussein Hassan Aly^a, Kunitada Shimotohno^b, Makoto Hijikata^{a,c,*}

^aLaboratory of Human Tumor Viruses, The Institute for Virus Research, Kyoto University, Department of Viral Oncology, 53 Kawaharacho, Shogoin, Sakyoku, Kyoto 606-8507, Japan

^bCenter for Human Metabolomic Systems Biology, Keio University, 35 Shinano-machi, Shinjuku-ku, Tokyo 160-8582, Japan

^cLaboratory of Viral Oncology, Graduate School of Biostudies, Kyoto University, Konocho, Yoshida, Sakyoku, Kyoto 606-8501, Japan

ARTICLE INFO

Article history:

Received 5 December 2008

Available online 25 December 2008

Keywords:

Hepatitis C virus

Infection

Replication

3D culture

PPAR

Immortalized hepatocytes

Blood-borne HCV

ABSTRACT

Due to the high polymorphism of natural hepatitis C virus (HCV) variants, existing recombinant HCV replication models have failed to be effective in developing effective anti-HCV agents. In the current study, we describe an *in vitro* system that supports the infection and replication of natural HCV from patient blood using an immortalized primary human hepatocyte cell line cultured in a three-dimensional (3D) culture system. Comparison of the gene expression profile of cells cultured in the 3D system to those cultured in the existing 2D system demonstrated an up-regulation of several genes activated by peroxisome proliferator-activated receptor alpha (PPAR α) signaling. Furthermore, using PPAR α agonists and antagonists, we also analyzed the effect of PPAR α signaling on the modulation of HCV replication using this system. The 3D *in vitro* system described in this study provides significant insight into the search for novel anti-HCV strategies that are specific to various strains of HCV.

© 2008 Elsevier Inc. All rights reserved.

Infection with Hepatitis C virus (HCV) is a serious health problem worldwide and leads to high rates of liver cirrhosis and hepatocellular carcinoma [1]. Given that the standard HCV therapy remains insufficient for the successful treatment of many patients [2], the development of more effective and less toxic anti-HCV agents is required. *In vitro* systems like the HCV replicon-bearing cells and the infectious particle-producing JFH1 system, has contributed to the discovery of new targets for anti-HCV therapy. However, these recombinant HCV genomes only proliferate in sublines of HuH-7 cells, which do not permit infection or proliferation of blood-borne HCV. Due to the high polymorphism of natural HCV, data from recombinant HCV systems could be evaluated by studying the therapeutic response of a variety of naturally occurring HCVs. However, the current systems available for such study remain insufficient due to the low infection and replication efficiency of the natural HCV strains.

More recently, production and secretion of infectious HCV particles has been reported in two independent three-dimensional (3D) cell culture systems, termed the radial-flow bioreactor (3D/RFB) and the thermoreversible gelatin polymer (3D/TGP) systems. These results were not observed in monolayer cultures [3],

suggesting that hepatocytes cultured in 3D more closely resemble liver cells *in vivo* [4] and thus support HCV proliferation. In addition, analysis of gene expression levels in 3D cultured cells revealed that the newly established immortalized human hepatocyte (HuS-E/2 cells) gene profile was altered to more closely resemble that of human liver tissue when the cells were cultured in 3D/TGP [5].

In the current study, we cultured HuS-E/2 cells in 3D/TGP and demonstrated efficient proliferation of natural HCV. Furthermore, gene expression analysis of these cells demonstrated the activation of the peroxisome proliferators-activated receptor α (PPAR α) signaling pathway, suggesting an important role for this pathway in the replication of natural HCV. Thus, the *in vitro* system described appears to be a useful tool for the study of HCV infection and proliferation as well as for the development of effective anti-viral agents against various natural HCVs.

Materials and methods

Cell culture. Immortalized human hepatocytes (HuS-E/2) and LucNeo#2 replicon cells [6] were cultured as previously described [5,7]. For the 3D-TGP culture system, 1×10^5 HuS-E/2 cells were cultured in 1 ml Mebiol gel (Mebiol Inc., Kanagawa, Japan)/well in 12-well plates. Five hundred microliters of fresh medium was overlaid on the solidified gel, and was changed every 2 days. Cell

* Corresponding author. Address: Laboratory of Human Tumor Viruses, The Institute for Virus, Kyoto University, Department of Viral Oncology, 53 Kawaharacho, Shogoin, Sakyoku, Kyoto 606-8507, Japan. Fax: +81 75 751 3998. E-mail address: mhijikat@virus.kyoto-u.ac.jp (M. Hijikata).

extraction from the gel was done at the designated time points according to the manufacturer's protocol.

RNA extraction, reverse transcriptase polymerase chain reaction (RT-PCR) and real-time RT-PCR (Q-PCR). At the designated time points, total cellular RNA was extracted and 1 μg of total RNA was used as a template for RT-PCR and for the quantitative detection of HCV-RNA using real-time RT-PCR (Q-PCR) as previously described [10].

HCV infection experiment. HCV infection experiments were carried out using sera from patients infected with HCV. Infection in 2D culture was undertaken as previously described [5]. For 3D/TGP cultured cells, the gel was solidified, and 50 μl HCV-containing patient serum with a titer of 1×10^6 HCV-RNA/ml was added to the culture and mixed. The culture was continued until the cells were extracted. Following extraction from 3D-TGP, cells were centrifuged and washed three times thoroughly with PBS. RNA was then extracted from the cells as described above. HCV infection into HuS-E/2 cells was also examined in the presence of anti-E2 mouse monoclonal antibody (917) as outlined previously [8].

Treatment of cells with PPAR α signaling agonists and antagonists. Fenofibrate or MK886 (Sigma–Aldrich, USA) were added to the culture medium of HuS-E/2 (2D-HuS-E/2) cells from day 0 of HCV infection; or the culture medium of LucNeo#2 replicon harboring cells. The cells were then cultured to the designated time point.

Microarray analysis. Gene expression profiles of 3D/TGP cultured HuS-E/2 cells were obtained by microarray analysis (3D-Genes Human 25, Toray, Tokyo, Japan) and compared to those of cells cultured in 2D.

Results

3D/TGP cultures enhance HCV proliferation in HuS-E/2 cells

Infection and proliferation of the HCV genotype 1b (HCV-RC5) derived from the serum of patient RC5 in HuS-E/2 cells cultured in 3D/TGP (3D/TGP-HuS-E/2 cells) was investigated and compared with that of HuS-E/2 cells cultured in 2D (2D-HuS-E/2). As outlined in Fig. 1A, the HCV-RNA levels in the 3D/TGP-HuS-E/2 cells were significantly higher at all of the time points examined following infection than in the 2D-HuS-E/2 cells, suggesting that the 3D/TGP system greatly enhances the proliferation of naturally occurring HCV in HuS-E/2 cells. Similar results were also obtained for sera from additional patients (data not shown). To examine whether the infection is viral envelope-receptor mediated, the infection experiments using serum treated with anti-HCV-E2 antibody (α -E2) or with anti-tubulin (negative control) was also performed. Pre-incubation of the serum with α -E2 significantly reduced the total amount of HCV-RNA in the cells upon infection (Fig. 1B). This result suggested that the infection of natural HCV into 3D/TGP-HuS-E/2 cells was HCV-E2-dependent.

Inhibition of natural HCV replication in HuS-E/2 cells by Interferon

In order to test the effects of anti-viral agents on natural HCV replication in 3D/TGP HuS-E/2 cells, 50–100 U/ml of IFN α was added to the medium overlaying the HCV-RC5 infected 3D/TGP-HuS-E/2 cells. The two treatment concentrations resulted in the inhibition of HCV-RNA replication in 3D-HuS-E/2 cells by

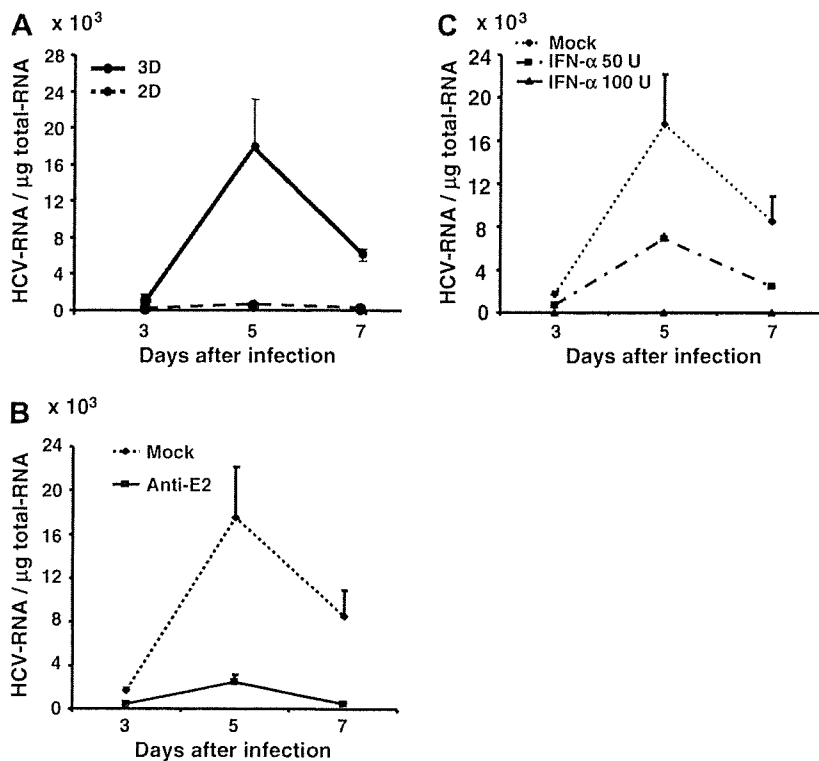


Fig. 1. HCV infection into 3D/TGP-HuS-E/2 cells. (A) 3D/TGP significantly enhanced HCV proliferation in HuS-E/2 cells. HCV patient serum was used to infect a similar number of HuS-E/2 cells cultured in 2D (hashed line) or 3D/TGP (solid line) culture for 24 h. Cells were then harvested and lysed at the indicated time points (3–7 days). The quantity of genomic HCV-RNA per 1 μg total RNA was determined by Q-PCR analysis. (B) Anti-E2 antibodies blocked HCV infection. HCV infection was performed as described in panel A in the presence of Anti-E2 specific or anti-tubulin (control) antibodies. (C) IFN α inhibits HCV replication in 3D/TGP-HuS-E/2 cells. HuS-E/2 cells were infected with HCV and fresh medium supplemented with or without (Mock), 50 U/ml, or 100 U/ml IFN α overlaid on the gel containing the cells and HCV proliferation measured as described above.

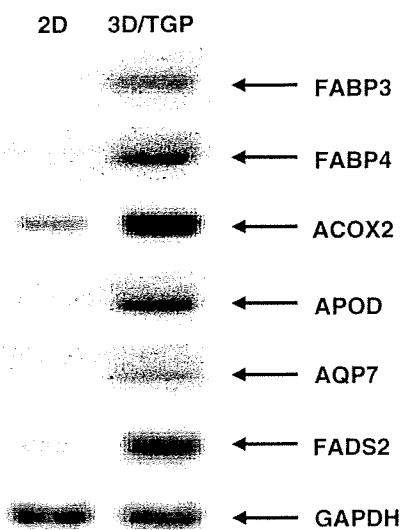


Fig. 2. RT-PCR analysis of the expression of genes identified by microarray. The PPAR α regulated genes were increased in 3D/TGP-HuS-E/2 cells (3D-TGP) and their expression levels measured by RT-PCR. 2D represents RNA samples from 2D-HuS-E/2 cells. Twenty cycles of amplification were undertaken for the RT-PCR analysis. GAPDH expression served as an internal control. *Abbreviations:* FABP3, fatty acid binding proteins 3; FABP4, fatty acid binding proteins 4; ACOX2, acyl-coenzyme A oxidase 2; APOD, apolipoprotein D; AQP7, aquaporin 7; FADS2, fatty acid desaturase 2; GAPDH, glyceraldehyde 3-phosphate dehydrogenase.

approximately 50–60% and almost completely, respectively, when compared to the replication in cells receiving mock treatment (Fig. 1C). These results demonstrate that the IFN α treatment was effective on HCV derived from RC5 and that 3D/TGP-HuS-E/2 cells may be useful for the screening of anti-HCV drugs for the treatment of natural HCV.

Increased activation of the PPAR α signaling pathway in 3D cultured HuS-E/2 cells

Given that 3D/TGP-HuS-E/2 cells demonstrated enhanced proliferation of natural HCV, the gene expression profiles of these cells was compared with that of cells cultured under normal 2D conditions using microarray analysis in order to identify the factors required for the enhanced proliferation. Among the 24,268 genes compared in this analysis, 212 genes demonstrated a greater than four folds index increase in expression in 3D/TGP than standard cultured cells. Cell signaling pathway analysis of these 212 genes showed that six genes, including fatty acid binding proteins 4 and 3 (FABP4 and 3), apolipoprotein D (APOD), aquaporin 7 (AQP7), acyl-coenzyme A oxidase 2 (ACOX2), and fatty acid desaturase 2 (FADS2), were targets of PPAR α signaling [9–12]. The increased expression of these genes in the 3D/TGP-HuS-E/2 cells was further confirmed by RT-PCR analysis (Fig. 2). Given that PPAR α is an essential factor for normal hepatocyte function [13], these results indicate that 3D/TGP culture enhances the hepatocyte-specific characteristics of HuS-E/2 cells.

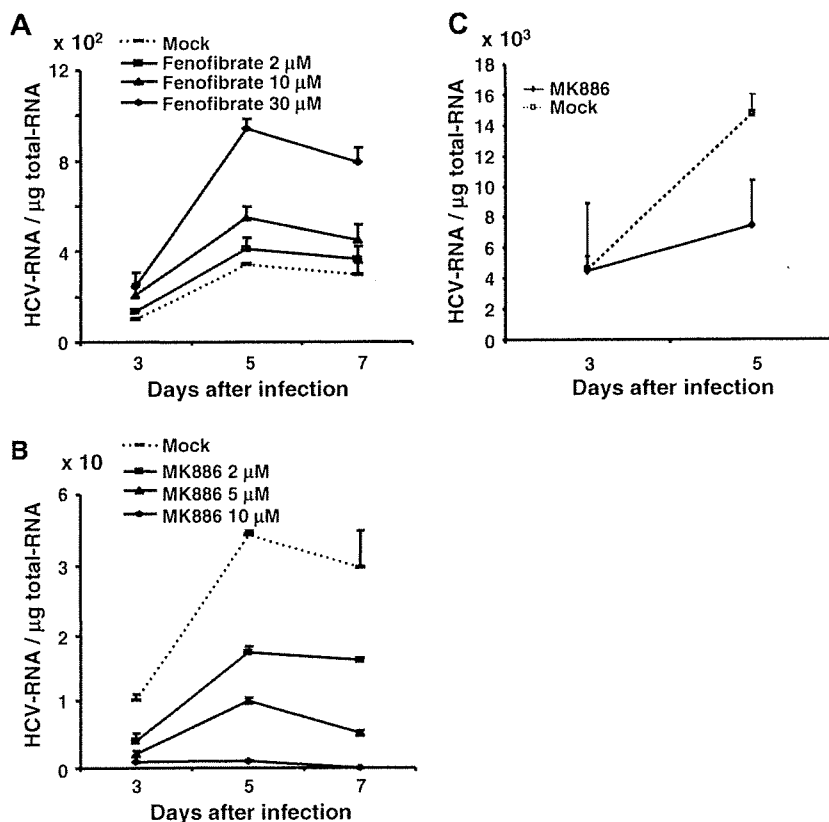


Fig. 3. The effects of PPAR α agonists and antagonists on natural HCV proliferation. (A) HuS-E/2 cells were infected with HCV and fresh medium supplemented with or without (Mock) 2, 10, or 30 μM of fenofibrate overlaid on the cells. (B) Medium supplemented with or without (Mock), 2, 5, or 10 μM of MK886 was overlaid on 2D-HuS-E/2 cells infected with HCV. HCV proliferation following treatment was measured by Q-PCR. (C) Medium supplemented with or without (Mock), 10 μM of MK886 was overlaid on 3D/TGP-HuS-E/2 cells infected with HCV. HCV proliferation following treatment was measured by Q-PCR.

PPAR α signaling affects HCV replication

We next examined the potential role of PPAR α signaling on HCV proliferation by monitoring HCV replication in 2D-HuS-E/2 cells that had been infected with HCV-RC5 and subsequently treated with the PPAR α agonist fenofibrate [14] or the PPAR α antagonist MK886 [14] (Fig. 3B). As outlined in Fig. 3A, a dose-dependent increase in HCV replication was observed in fenofibrate-treated cells. In contrast, a dose-dependent decrease in HCV proliferation was observed in the presence of MK886. Similarly, treatment with MK886 reduced HCV proliferation in 3D/TGP-HuS-E/2 cells (Fig. 3C). The response of HCV proliferation in response to fenofibrate and MK886 treatment was also analyzed in LucNeo#2 cells that contained HCV replicon RNA (LNMH14) derived from the HCV-1b genome (Fig. 4A). Luciferase expression in these cells represented replication of the HCV replicon [6] and, as shown in Fig. 4A, luciferase activity in the cells treated with fenofibrate or MK886 also showed either enhancement or suppression of replicon proliferation, respectively. In addition, the increased HCV replication following fenofibrate treatment was completely abolished when treated with MK886 simultaneously. As MK886 is known to induce apoptosis when administered in high doses [15], the cell viability

was examined using the XTT assay. There were no significant effects on cell viability after treatment with fenofibrate. Although MK886 resulted in a minor reduction in XTT values when high doses (10–15 μ M) were administered, this reduction was not statistically significant when compared to its effect on HCV replication (Fig. 4B). This result suggests that PPAR α signaling is required for HCV replication and that suppression of PPAR α signaling has an anti-HCV effect.

Discussion

In the current study, we demonstrated that immortalized hepatocyte HuS-E/2 cells cultured in 3D/TGP support the infection and replication of natural HCV derived from patient sera. Unlike recombinant HCVs, which have been required to adapt to sublines of HuH-7 cells [16], the population of the natural HCV is fairly polymorphic, demonstrating different responses to a variety of anti-viral agents [17,18]. The 3D/TGP-HuS-E/2 cells have the advantage of being a small-scale 3D cultured cells, which are cultured in 12-well plates at a density of 1×10^5 /well, that allow the study of both viral and cellular events. In the current study, it demonstrated a 2 log increase in susceptibility to natural HCV infection and replication when compared to conventional 2D culture systems. Thus it offers an important advantage in the study of natural HCV infection and replication, and the response of natural HCV to anti-HCV drugs.

As the ability of HuS-E/2 cells to support infection and replication of natural HCV was greatly altered by the culture conditions, it is likely that the culture system described in our study will provide important information in regards to the cellular factors that support the HCV life cycle. The microarray study showed that the expression of some genes related to the PPAR α signaling pathway were upregulated in the 3D cultured HuS-E/2 cells. Using both PPAR α signaling agonists and antagonists, PPAR α signaling was shown to affect infection and proliferation of natural HCV. PPAR α is a ligand-activated transcription factor that is primarily expressed in tissues with high lipid metabolism including the liver, where it functions as one of three major nuclear receptors and is essential for its normal function [19]. Similar to a part of our data, a negative effect on HCV replication was previously observed in the replicon-bearing cells treated with siRNA for PPAR α , with only 50% reduction of HCV-RNA [20]. In this study, even a large dose of PPAR α agonist enhanced natural HCV replication in the 2D-HuS-E/2 cells for three times, despite the 2 logs enhancement of HCV proliferation in 3D/TGP culture. This implies that additional factors activated in 3D/TGP-HuS-E/2 cells may be required for the efficient HCV proliferation. Further analysis of the microarray data may provide us with further information on factors that may prove useful in the development of anti-HCV drugs.

In conclusion, the novel *in vitro* culture system combining TGP and immortalized hepatocytes described in this study demonstrated efficient support of natural HCV infection and replication. This system may be used in future virological studies to define new anti-HCV strategies. It may also prove useful for the specific design of effective individual therapy according to patient-specific strains.

Acknowledgments

This work was supported by Grants-in-Aid from the Ministry of Health, Labor and Welfare of Japan; and for scientific research from Ministry of Education, Sports, Culture, and Technology of Japan.

References

- [1] Z. Younossi, J. Kallman, J. Kincaid, The effects of HCV infection and management on health-related quality of life, *Hepatology* 45 (2007) 806–816.

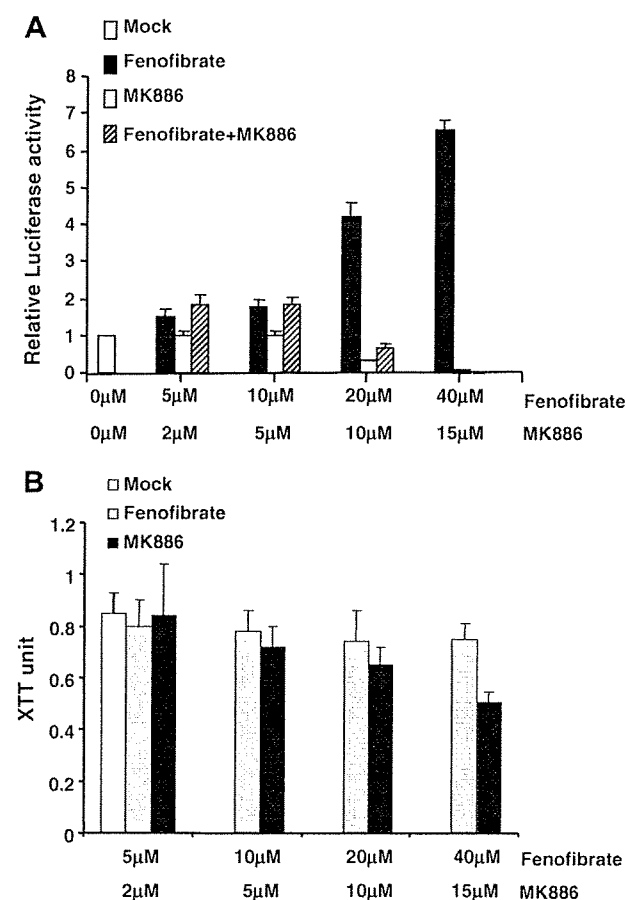


Fig. 4. The effects of PPAR α agonists and antagonists on the replication of HCV subgenomic replicons. (A) LucNeo#2 cells containing a HCV subgenomic replicon termed LNMH14, were mock treated or treated with fenofibrate, MK886, or a combination of both fenofibrate and MK886 at the indicated concentrations for 2 days. Luciferase activity derived from the replicon was then measured as an indicator of HCV replication [7]. (B) Following treatment with fenofibrate and MK886, LucNeo#2 cells were cultured for 2 days and cell viability measured using the XTT assay (Roche, Mannheim, Germany).

- [2] M.W. Fried, M.L. Shiffman, K.R. Reddy, C. Smith, G. Marinos, F.L. Goncales Jr., D. Haussinger, M. Diago, G. Carosi, D. Dhumeaux, A. Craxi, A. Lin, J. Hoffman, J. Yu, Peginterferon alfa-2a plus ribavirin for chronic hepatitis C virus infection, *N. Engl. J. Med.* 347 (2002) 975–982.
- [3] K. Murakami, K. Ishii, Y. Ishihara, S. Yoshizaki, K. Tanaka, Y. Gotoh, H. Aizaki, M. Kohara, H. Yoshioka, Y. Mori, N. Manabe, I. Shoji, T. Sata, R. Bartenschlager, Y. Matsuura, T. Miyamura, T. Suzuki, Production of infectious hepatitis C virus particles in three-dimensional cultures of the cell line carrying the genome-length dicistronic viral RNA of genotype 1b, *Virology* 351 (2006) 381–392.
- [4] G. Andrei, Three-dimensional culture models for human viral diseases and antiviral drug development, *Antiviral Res.* 71 (2006) 96–107.
- [5] H.H. Aly, K. Watashi, M. Hijikata, H. Kaneko, Y. Takada, H. Egawa, S. Uemoto, K. Shimotohno, Serum-derived hepatitis C virus infectivity in interferon regulatory factor-7-suppressed human primary hepatocytes, *J. Hepatol.* 46 (2007) 26–36.
- [6] K. Goto, K. Watashi, T. Murata, T. Hishiki, M. Hijikata, K. Shimotohno, Evaluation of the anti-hepatitis C virus effects of cyclophilin inhibitors, cyclosporin A, and NIM811, *Biochem. Biophys. Res. Commun.* 343 (2006) 879–884.
- [7] T. Murata, M. Hijikata, K. Shimotohno, Enhancement of internal ribosome entry site-mediated translation and replication of hepatitis C virus by PD98059, *Virology* 340 (2005) 105–115.
- [8] M.A. El-Farrash, H.H. Aly, K. Watashi, M. Hijikata, H. Egawa, K. Shimotohno, In vitro infection of immortalized primary hepatocytes by HCV genotype 4a and inhibition of virus replication by cyclosporin, *Microbiol. Immunol.* 51 (2007) 127–133.
- [9] J. Samulin, I. Berget, S. Lien, H. Sundvold, Differential gene expression of fatty acid binding proteins during porcine adipogenesis, *Comp. Biochem. Physiol. B: Biochem. Mol. Biol.* 151 (2008) 147–152.
- [10] S. Hummasti, B.A. Laffitte, M.A. Watson, C. Galardi, L.C. Chao, L. Ramamurthy, J.T. Moore, P. Tontonoz, Liver X receptors are regulators of adipocyte gene expression but not differentiation: identification of apoD as a direct target, *J. Lipid Res.* 45 (2004) 616–625.
- [11] C.G. Walker, M.J. Holness, G.F. Gibbons, M.C. Sugden, Fasting-induced increases in aquaporin 7 and adipose triglyceride lipase mRNA expression in adipose tissue are attenuated by peroxisome proliferator-activated receptor alpha deficiency, *Int. J. Obes. (Lond.)* 31 (2007) 1165–1171.
- [12] D.G. Jump, D. Botolin, Y. Wang, J. Xu, B. Christian, O. Demeure, Fatty acid regulation of hepatic gene transcription, *J. Nutr.* 135 (2005) 2503–2506.
- [13] D.W. Crabb, S. Liangpunsakul, Alcohol and lipid metabolism, *J. Gastroenterol. Hepatol.* 21 (Suppl. 3) (2006) S56–S60.
- [14] D. Panigrahy, A. Kaipainen, S. Huang, C.E. Butterfield, C.M. Barnes, M. Fannon, A.M. Laforme, D.M. Chaponis, J. Folkman, M.W. Kieran, PPARalpha agonist fenofibrate suppresses tumor growth through direct and indirect angiogenesis inhibition, *Proc. Natl. Acad. Sci. USA* 105 (2008) 985–990.
- [15] V.S. Deshpande, J.P. Kehrer, Mechanisms of *N*-acetylcysteine-driven enhancement of MK886-induced apoptosis, *Cell Biol. Toxicol.* 22 (2006) 303–311.
- [16] K.J. Blight, A.A. Kolykhalov, C.M. Rice, Efficient initiation of HCV RNA replication in cell culture, *Science* 290 (2000) 1972–1974.
- [17] R.C. Dickson, Clinical manifestations of hepatitis C, *Clin. Liver Dis.* 1 (1997) 569–585.
- [18] E.J. Heathcote, Antiviral therapy: chronic hepatitis C, *J. Viral Hepat.* 14 (Suppl. 1) (2007) 82–88.
- [19] C.N. Palmer, M.H. Hsu, K.J. Griffin, J.L. Raucy, E.F. Johnson, Peroxisome proliferator activated receptor-alpha expression in human liver, *Mol. Pharmacol.* 53 (1998) 14–22.
- [20] B. Rakic, S.M. Sagan, M. Noestheden, S. Belanger, X. Nan, C.L. Evans, X.S. Xie, J.P. Pezacki, Peroxisome proliferator-activated receptor alpha antagonism inhibits hepatitis C virus replication, *Chem. Biol.* 13 (2006) 23–30.

A Genetic Variant of Hepatitis B Virus Divergent from Known Human and Ape Genotypes Isolated from a Japanese Patient and Provisionally Assigned to New Genotype J[†]

Kanako Tatematsu,¹ Yasuhito Tanaka,^{1*} Fuat Kurbanov,¹ Fuminaka Sugauchi,²
Shuhei Mano,³ Tatsuji Maeshiro,⁴ Tomokuni Nakayoshi,⁵ Moriaki Wakuta,⁶
Yuzo Miyakawa,⁷ and Masashi Mizokami^{1,8}

Department of Clinical Molecular Informative Medicine¹ and Department of Gastroenterology and Metabolism,² Nagoya City University Graduate School of Medical Sciences, Nagoya, Japan; Nagoya City University Graduate School of Natural Sciences, Nagoya, Japan³; Control and Prevention of Infectious Diseases, Department of Medicine and Therapeutics, Faculty of Medicine, University of the Ryukyus, Okinawa, Japan⁴; Heart Life Hospital, Okinawa, Japan⁵; Wakusan Clinic, Okinawa, Japan⁶; Miyakawa Memorial Research Foundation, Tokyo, Japan⁷; and Research Center for Hepatitis and Immunology, International Medical Center of Japan Kohnodai Hospital, Chiba, Japan⁸

Received 5 March 2009/Accepted 24 July 2009

Hepatitis B virus (HBV) of a novel genotype (J) was recovered from an 88-year-old Japanese patient with hepatocellular carcinoma who had a history of residing in Borneo during the World War II. It was divergent from eight human (A to H) and four ape (chimpanzee, gorilla, gibbon, and orangutan) HBV genotypes, as well as from a recently proposed ninth human genotype I, by 9.9 to 16.5% of the entire genomic sequence and did not have evidence of recombination with any of the nine human genotypes and four nonhuman genotypes. Based on a comparison of the entire nucleotide sequence against 1,440 HBV isolates reported, HBV/J was nearest to the gibbon and orangutan genotypes (mean divergences of 10.9 and 10.7%, respectively). Based on a comparison of four open reading frames, HBV/J was closer to gibbon/orangutan genotypes than to human genotypes in the P and large S genes and closest to Australian aboriginal strains (HBV/C4) and orangutan-derived strains in the S gene, whereas it was closer to human than ape genotypes in the C gene. HBV/J shared a deletion of 33 nucleotides at the start of preS1 region with C4 and gibbon genotypes, had an S-gene sequence similar to that of C4, and expressed the *ayw* subtype. Efficient infection, replication, and antigen expression by HBV/J were experimentally established in two chimeric mice with the liver repopulated for human hepatocytes. The HBV DNA sequence recovered from infected mice was identical to that in the inoculum. Since HBV/J is positioned phylogenetically in between human and ape genotypes, it may help to trace the origin of HBV and merits further epidemiological surveys.

Worldwide, an estimated 400 million people are infected with hepatitis B virus (HBV) persistently, of whom three quarters live in the Southeast and Far East Asia, and one million die of decompensated cirrhosis and/or hepatocellular carcinoma (HCC) annually (8, 15). HBV is the smallest animal DNA virus and has a genome made of approximately 3,200 nucleotides (nt) that contains four open reading frames for P, C, S, and X genes; they code for DNA polymerase/reverse-transcriptase, core protein, surface protein, and X protein, respectively (49). The S gene is divided into preS1 and preS2 regions and the small S gene, and the C gene splits into PreC and C.

Eight genotypes of HBV have been recognized by a sequence divergence of >8% in the entire genome and named by capital alphabet letters (A to H) in the order of discovery (3, 26, 29, 42). HBV genotypes are further classified into subgenotypes, such as B1/Bj and B2-5/Ba (44), as well as C1/Cs, C2/Ce,

and C3-5 (36). A systematic nomenclature is proposed for designating HBV subgenotypes using Arabic numbers, such as A1, A2, and A3 (25). HBV genotypes have distinct geographical distribution (16, 23). Genotype A is prevalent in Africa, Europe and India, genotypes B and C are common in Asia, and genotype E is common in sub-Saharan Africa. Genotypes F and H are restricted to Central and South American continents, whereas genotype D is distributed all over the world. HBV genotypes have clinical application, and they influence severity and progression of liver disease and the response to antiviral therapies. Previous reports indicate that HCC is more frequent in the patients infected with genotype C than B (7, 47), and interferon is more effective in those infected with genotype B than C in Asia and more effective in those infected with genotype A than D in Europe (18, 34, 51).

Recently, a ninth genotype (I) was tentatively proposed for HBV strains detected in Laos (31). These strains are phylogenetically similar to aberrant Vietnamese strains that display complex recombination over the genome (10). In the present study, an HBV isolate was recovered from a Japanese patient with HCC, who was involved in military actions in Borneo during the World War II. The isolated strain was compared against eight human (A to H) and four ape (chimpanzee, gorilla, gibbon, and orangutan) genotypes and was provisionally designated genotype J. The new genotype was assigned based on a sequence diver-

* Corresponding author. Mailing address: Department of Clinical Molecular Informative Medicine, Nagoya, City University Graduate School of Medical Sciences, Kawasumi, Mizuho, Nagoya 467-8601, Japan. Phone: (81) 52-853-8292. Fax: (81) 52-842-0021. E-mail: ytanaka@med.nagoya-cu.ac.jp.

† Supplemental material for this article may be found at <http://jvi.asm.org/>.

‡ Published ahead of print on 29 July 2009.

TABLE 1. Nucleotide divergence in the full-genome sequence estimated from pairwise comparison between the Ryukyus 34 strain of a provisional genotype J and 1,440 HBV strains from the database entered by September 2008

Genotype	No. of strains	Divergence (%)		
		Range	Mean	SD
A	202	12.1–15.9	13.0	0.4
B	309	11.1–13.6	11.9	0.5
C	396	11.2–13.1	11.9	0.5
D	264	12.6–15.0	13.4	0.2
E	90	12.3–13.4	12.7	0.3
F	56	15.2–16.5	15.6	0.2
G	23	12.8–14.6	13.7	0.3
H	21	15.4–16.3	15.7	0.3
I	16	11.4–12.0	11.7	0.2
Chimpanzee	14	11.6–12.7	12.1	0.3
Gorilla	1	12.2		
Gibbon	34	9.9–11.7	10.9	0.5
Orangutan	12	10.4–11.2	10.7	0.4
Woolly monkey	2	27.2–27.4	27.3	0.1

gence of 10.7 to 15.7% from other genotypes, a unique phylogenetic position between human and ape genotypes, and the absence of strong evidence of recombination.

MATERIALS AND METHODS

Patient. A Japanese man, 88 years old, developed HCC in 2006. He had a history of residing in Borneo during the World War II. No HBV infections were recorded in his family members. In October 1996, he was diagnosed with chronic hepatitis B. Hepatitis B surface antigen (HBsAg) was detected in serum, and the aspartate aminotransferase and alanine aminotransferase levels were elevated to 83 and 73 U/liter, respectively (normal levels, <30 U/liter for both). Thereafter, the transaminase levels were normalized, and he had been monitored as an asymptomatic HBV carrier. In August 2000, the level of a tumor marker (des- γ -carboxy prothrombin) was elevated to 52 mAU/ml (normal, <40 mAU/ml), while another tumor marker (alpha-fetoprotein) remained within normal range (<10 ng/ml) as alanine aminotransferases. In October 2006, a tumor (4.3 by 4.1 cm) was detected in the liver by ultrasonography, and he received treatment with transarterial embolization. Des- γ -carboxy prothrombin was elevated to 419 mAU/ml, while the aminotransferase levels remained within normal limits. Hepatitis B e antigen (HBeAg) was negative, and the corresponding antibody (anti-HBe) was detected in his serum. The subtype of HBsAg in this serum was *ayw*.

HBV DNA was extracted from his serum specimen obtained in 2006, and the full-length genome sequence was determined for phylogenetic and biological analyses. An informed consent had been obtained from the patient, and the study protocol conforms to the ethical guidelines of the 1975 Declaration of Helsinki as reflected in a priori approval by the institution's human research committee.

Markers of HBV infection. HBeAg and anti-HBe were determined by enzyme-linked immunosorbent assay (ELISA) with commercial kits (HBeAg EIA; Institute of Immunology, Tokyo, Japan), and subtypes of HBsAg by ELISA with commercial kits (HBsAg Subtype EIA; Institute of Immunology). Hepatitis B core-related antigen (HBcrAg) was determined by chemiluminescence enzyme immunoassay (13). The method allows more sensitive detection of core protein and, as was shown in previous studies, HBcrAg levels reflect HBV DNA loads and well correlate with intrahepatic covalently closed circular DNA (cccDNA) levels. The measurement of serum HBcrAg is a useful noninvasive tool for monitoring intrahepatic HBV viral status (52). HBV DNA was quantified by the S gene-targeted real-time detection PCR with a sensitivity of 100 copies/ml (equivalent to 20 IU/ml) (1). However, due to small volumes of sera available from the challenged mice, HBV DNA was extracted from 10-fold-diluted specimens, resulting in reduced assay sensitivity in the present study (1,000 copies/ml [200 IU/ml]).

Determination of the complete nucleotide sequence of HBV/J isolate. HBV DNA was extracted by using the QIAamp DNA blood kit (Qiagen, GmbH, Hilden, Germany) from 100 μ l of serum that had been stored at -80°C . The complete genome sequence of an HBV/J isolate recovered from the patient was determined by the strategy previously reported (43). In brief, two sets of primers were designed to amplify overlapping fragments (A and B) covering the entire

HBV genome (stat not shown). Nested PCR was carried out for 35 cycles (95°C , 30 s; 57°C , 30 s; and 72°C , 2 min) using TaKaRa LA *Taq* polymerase (Takara Biochemicals, Kyoto, Japan). Amplified fragments were inserted into the pGEM-T Easy vector (Promega, Madison, WI), and cloned in DH5a cells (Toyobo, Osaka, Japan). Obtained HBV DNA clones were confirmed to have the sequence identical to the major-clone consensus sequence determined directly on PCR products by Prism BigDye (Applied Biosystems, Foster City, CA) in the ABI 3100 automated sequencer.

Phylogenetic analysis. Full-length sequences of HBV isolates were aligned with use of the CLUSTAL W software program (48) (available at www.ebi.ac.uk), and the alignment was confirmed by visual inspection. Genetic distances were estimated by the six-parameter method, and phylogenetic trees were constructed with the neighbor-joining method (35). To confirm the reliability of phylogenetic trees, bootstrap resampling and reconstruction were carried out 1,000 times using the program

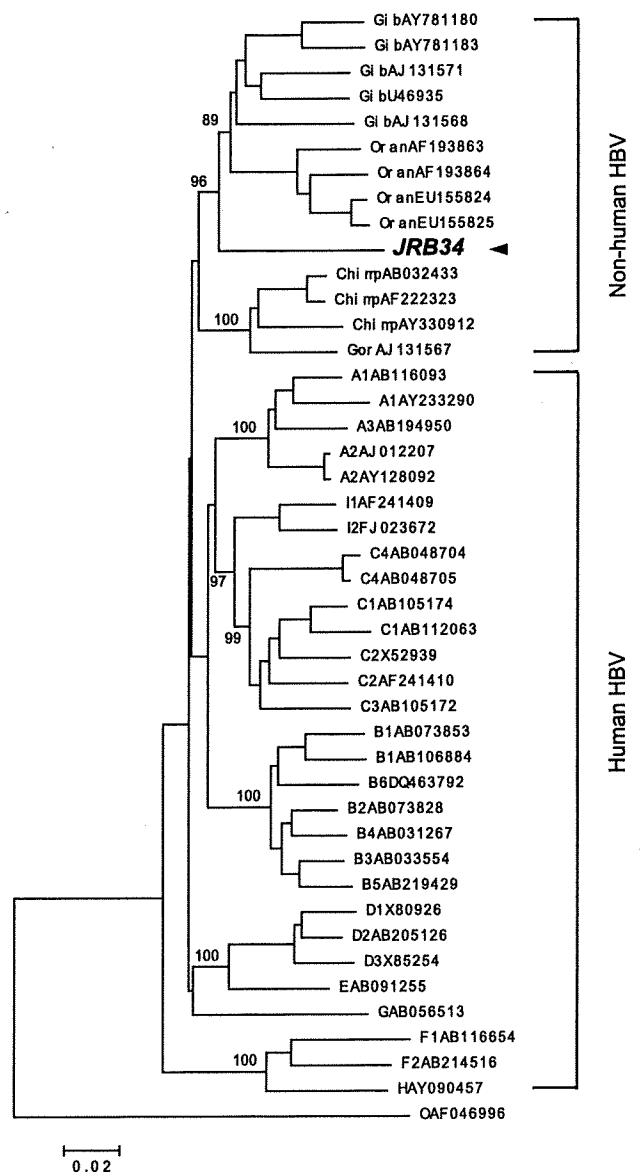


FIG. 1. Phylogenetic tree constructed on the entire genome sequences of 44 HBV isolates representing four ape and eight human genotypes. A woolly monkey HBV isolate serves as an outgroup. The HBV/J isolate (JRB34) is indicated by an arrowhead, and the genetic distance is indicated by a bar below.

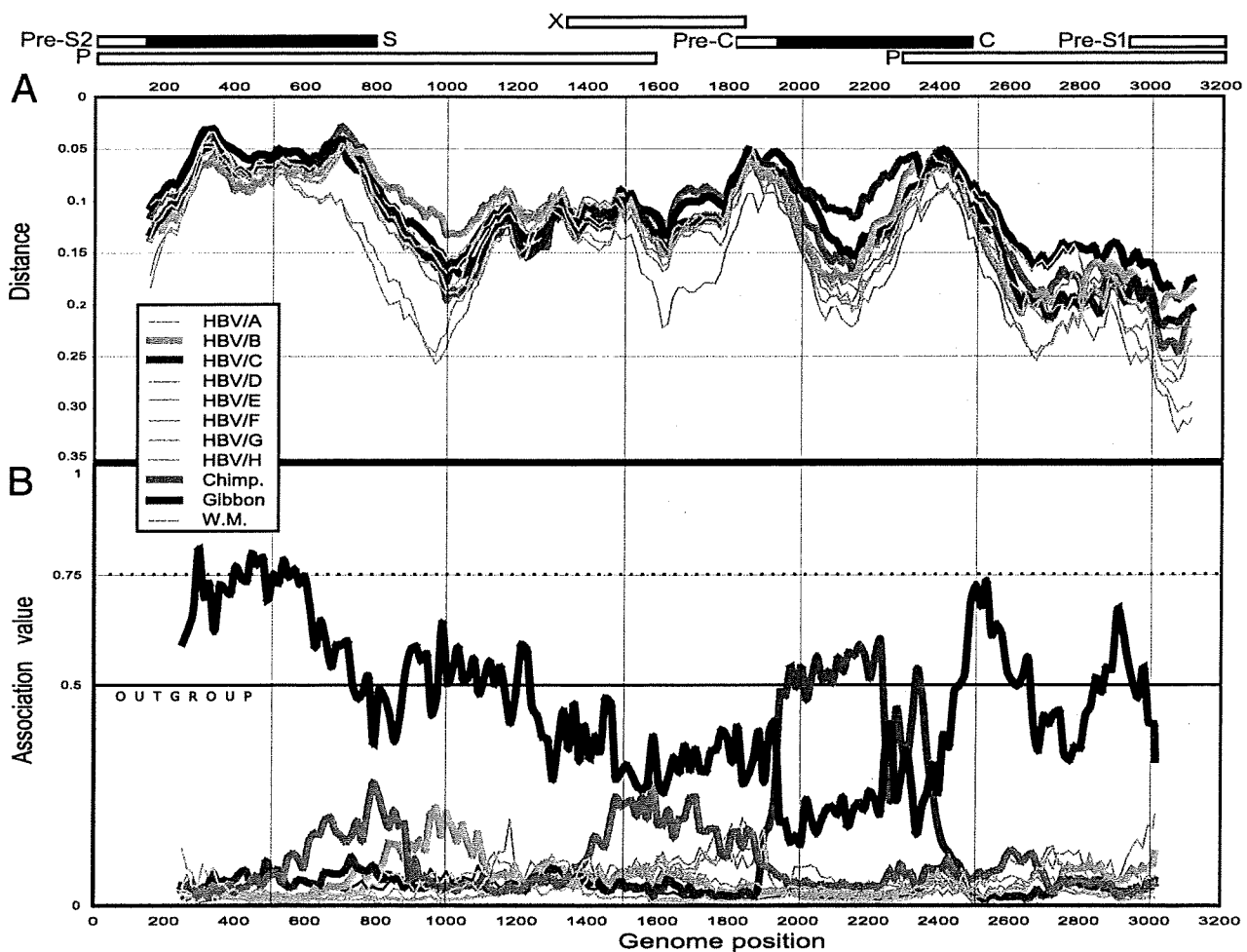


FIG. 2. Complete genome scanning carried by PHYLIP, the phylogeny inference package implemented in the Simmonic software, for the JRB34 strain versus 228 selected nonrecombinant HBV genotypes (HBV/Ba and HBV/I not included) reference strains grouped by genotype. Kimura two-parameter distance model (A) and grouping scan (B) were determined with a 300-nt size window sliding by an increment of 15 nucleotides. The x axis indicates the genome position (corresponding to the midpoint of the scanning fragment), and the y axis indicates the mean distances between JRB34 and reference groups (A). Phylogenetic association (y axis) was evaluated throughout entire HBV genome (x axis) with the same window and step size parameters (B). The association value below 0.5 was considered to represent an outgroup. The open reading frame map is shown schematically at the top of the figure.

of the Hepatitis Virus Database (39). All 1,440 complete genomes available in the DDBJ/GenBank served as references for the initial alignment in the present study. Divergence in the nucleotide sequence between a strain of provisional genotype J and previously reported strains was estimated by using MEGALIGN v.6.00 (Lazer-gene package; DNASTAR, Inc., Madison, WI).

Examination of recombination evidence. Evidence of possible recombination was investigated by using the software packages Simmonic 2005 v1.6 and SimPlot v3.5.1, both implementing PHYLIP (Phylogeny Inference Package v3.68; J. Felsenstein, Department of Genome Sciences, University of Washington, Seattle [distributed by the authors]) (19, 40).

Inoculation of chimeric mice with the liver repopulated for human hepatocytes. Severe combined immunodeficiency mice transgenic for the urokinase-type plasminogen activator gene ($uPA^{+/+}/SCID^{+/+}$ mice) with the liver repopulated with human hepatocytes (chimeric mice) were purchased from Phoenix Bio Co., Ltd. (Hiroshima, Japan). Human serum albumin was measured by ELISA with commercial assay kits (Eiken Chemical Co., Ltd., Tokyo, Japan) for estimating the extent of repopulation. The research complied with all relevant federal guidelines and institutional policies.

Immunofluorescence. Freshly prepared liver tissues were snap-frozen in isopentane precooled in liquid nitrogen. Frozen specimens were cut at 5 to 6 μ m by cryostat, mounted on glass slides, air dried, and fixed in 100% acetone at room

temperature for 10 min. Sections were blocked with antibody diluent (Dako, Tokyo, Japan) and stained for hepatitis B core antigen (HBcAg). They were incubated with rabbit anti-HBc (Dako) at room temperature for 1 h, washed in phosphate-buffered saline, and then incubated with goat anti-rabbit immunoglobulin G conjugated with Cy3 (Chemicon International, Inc., Temecula, CA) or goat anti-human albumin antibody labeled with fluorescein isothiocyanate (Bethyl Laboratories, Inc., Montgomery, TX). Sections were washed with phosphate-buffered saline and observed in a fluorescence microscope (Eclipse E800M; Nikon, Tokyo, Japan).

Nucleotide sequence accession numbers. The nucleotide sequence data reported in the present study will appear in the DDBJ/EMBL/GenBank databases under accession no. AB486012.

RESULTS

Composition of the HBV genome of genotype J. HBV DNA was extracted from serum of a patient with HCC. It was named JRB34 ("J" for Japanese; "R" after the southernmost island [Ryukyu] where the patient has spent most of his life now

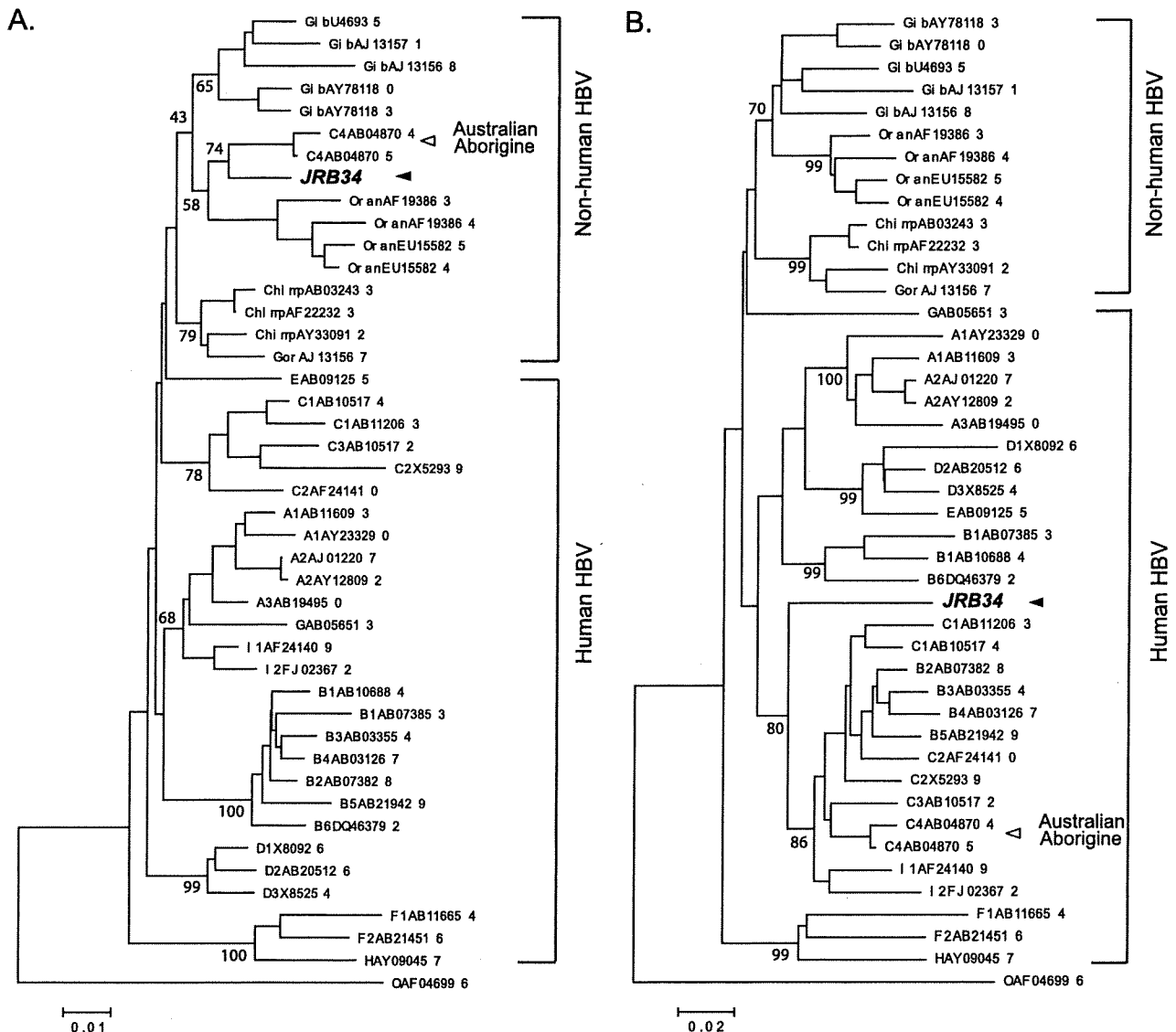


FIG. 3. Phylogenetic tree constructed on the preS/S gene (A) and C gene (B) sequences of 44 HBV isolates representing four ape and eight human genotypes. A woolly monkey HBV isolate serves as an outgroup. The HBV/J isolate (JRB34) is indicated by an arrowhead, and an HBV/C4 isolate from Australian aborigine is indicated by an open triangle. The genetic distance is indicated by a bar below.

Downloaded from jvi.asm.org at NAGOYA CITY UNIV LIB on September 23, 2009

exceeding 90 years; and “B” for Borneo where he is suspected to have contracted the HBV infection). The entire nucleotide sequence was determined for the JRB34 isolate of genotype J (HBV/J). It had a genomic length of 3,182 nt, which consisted of envelope gene containing preS1 region (nt 2848 to 3171, coding for 108 amino acids [aa]), preS2 region (nt 3172 to 154 [55 aa]), and the small S gene (nt 155 to 835 [226 aa]), X gene (nt 1374 to 1838 [154 aa]), preC region (nt 1814 to 1897 [27 aa]), C gene (nt 1901 to 2452 [183 aa]), and P gene (nt 2307 to 1623 [832 aa]).

Sequence divergence of the JRB34 strain from other genotypes. The complete genome sequence of the JRB34 strain obtained in the present study was compared against those of 1,440 HBV genomes registered in the Viral Hepatitis Database

(39). Estimated nucleotide sequence divergence of the JRB34 strain from four ape and nine human genotypes is summarized in the Table 1. The mean divergence by genotypes ranged from 10.7 and 10.9% (from orangutan and gibbon, respectively) to 15.6 and 15.7% (from genotypes F and H, respectively). Surprisingly, the minimum divergence of 9.9% was observed in comparison with a nonhuman HBV isolate from *Hilobates agilis* gibbon confiscated in Taiwan in 1993 (AY330917) (41). Since the sequence divergence from any documented genotypes, including recently proposed genotype I, exceeded 8%, the JRB34 strain was tentatively classified into a novel genotype J of HBV.

Phylogenetic analysis of the entire genomic sequence. In the phylogenetic tree constructed on 1,440 complete genome

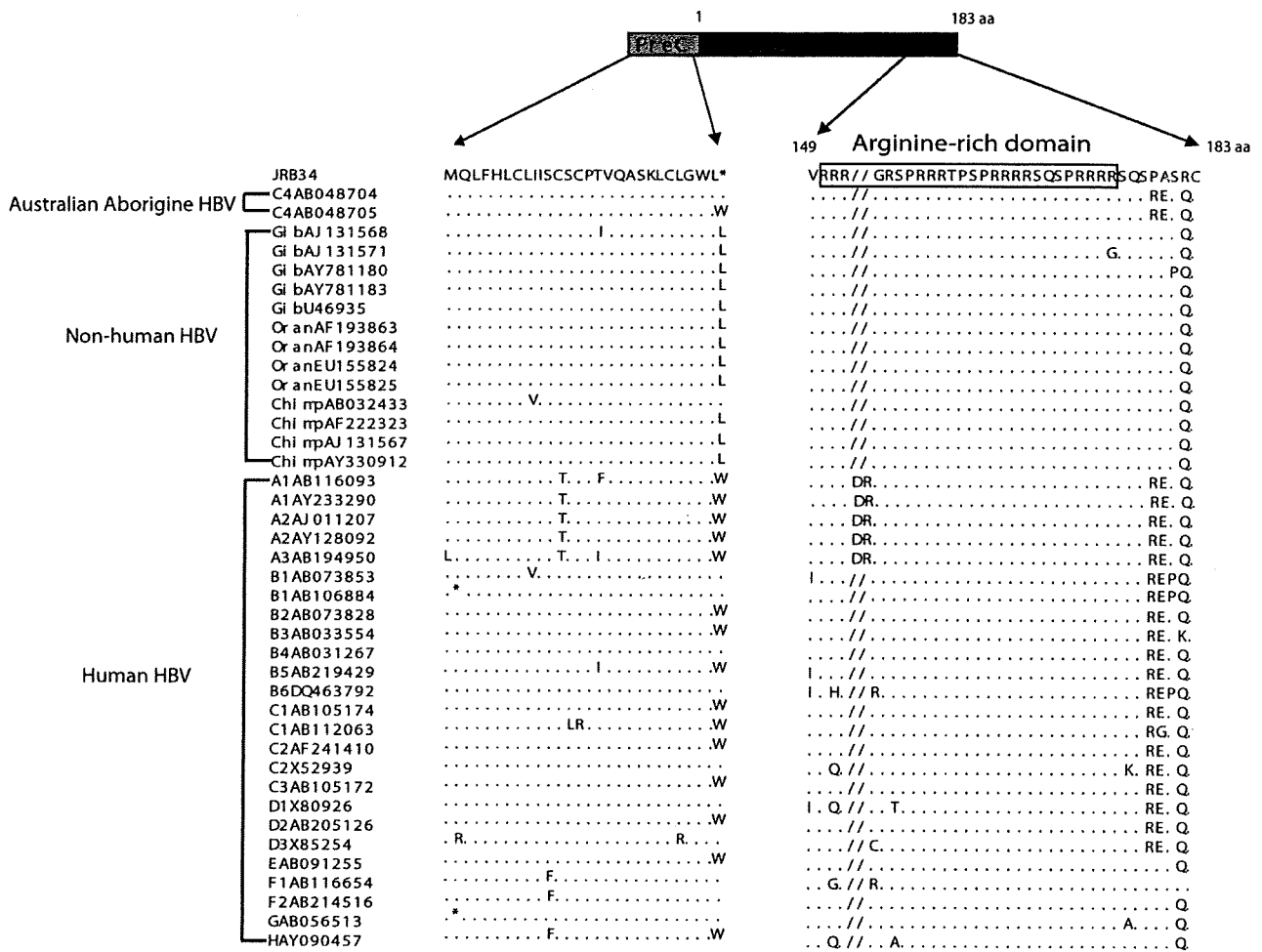


FIG. 4. Comparison of the amino acid sequence in the preC gene and carboxy-terminal amino acid sequences in the C gene of HBV isolates of various genotypes. The sequence of the HBV/J isolate (JRB34) is indicated at the top. Dots represent amino acids shared by JRB34, and a dash indicates the deletion of an amino acid. The sequence of the arginine-rich domain bearing the binding site with HBV DNA is boxed.

EMBL/DDBJ/GenBank database entries, the HBV/J strain was positioned distinctively from all known human genotypes (data not shown). It was closest to the cluster formed by gibbon- and orangutan-derived strains. However, including recombinant strains in such analyses may significantly affect the overall phylogenetic topology. This possibility was ruled out by reconstruction of the phylogeny using nonrecombinant HBV strains that further confirmed the phylogenetic peculiarity of the studied JRB34 strain (see Fig. S1 in the supplemental material). A total of 44 representative reference strains were further selected for establishing the consistency. Thus, phylogenetic topology indicating genotype-specific clustering is shown in the Fig. 1. Hence, using various sets of references, we confirmed that genotype J undoubtedly differed phylogenetically from all other known genotypes.

Lack of significant evidence of recombination with other human or ape genotypes in genotype J. To investigate possible recombination in the JRB34 genome, a window scanning analysis of aligned HBV genomes was performed by means of Simplot and Simmonics software packages. Both Bootscanning

by SimPlot and GroupScanning by Simmonics showed similar output results. However, the methodological approach is different between these two software packages; GroupScanning provides more robust analysis of the phylogenetic relation between the examined strain and clusters of reference strains, whereas SimPlot does this comparison between the examined strain and parametrically generated consensus of the reference strains. The results obtained by SimPlot therefore can be significantly affected by selected parameters for the generation of consensus. This is especially undesirable when a new genotype strain (for which no references are available among known genotypes) is being analyzed (40). Figure 2 shows genome-wide distance scanning and GroupScanning plots for the JRB34 strain in comparison with a reference set consisting of 228 nonrecombinant HBV isolates retrieved from the public database (the phylogenetic tree is shown in Fig. S1 in the supplemental material). It is evident that the JRB34 strain was divergent from all known genotypes, and the closest genetic neighbors were estimated by distance and phylogenetic association scanning were the gibbon genotype (in preS, S, and P

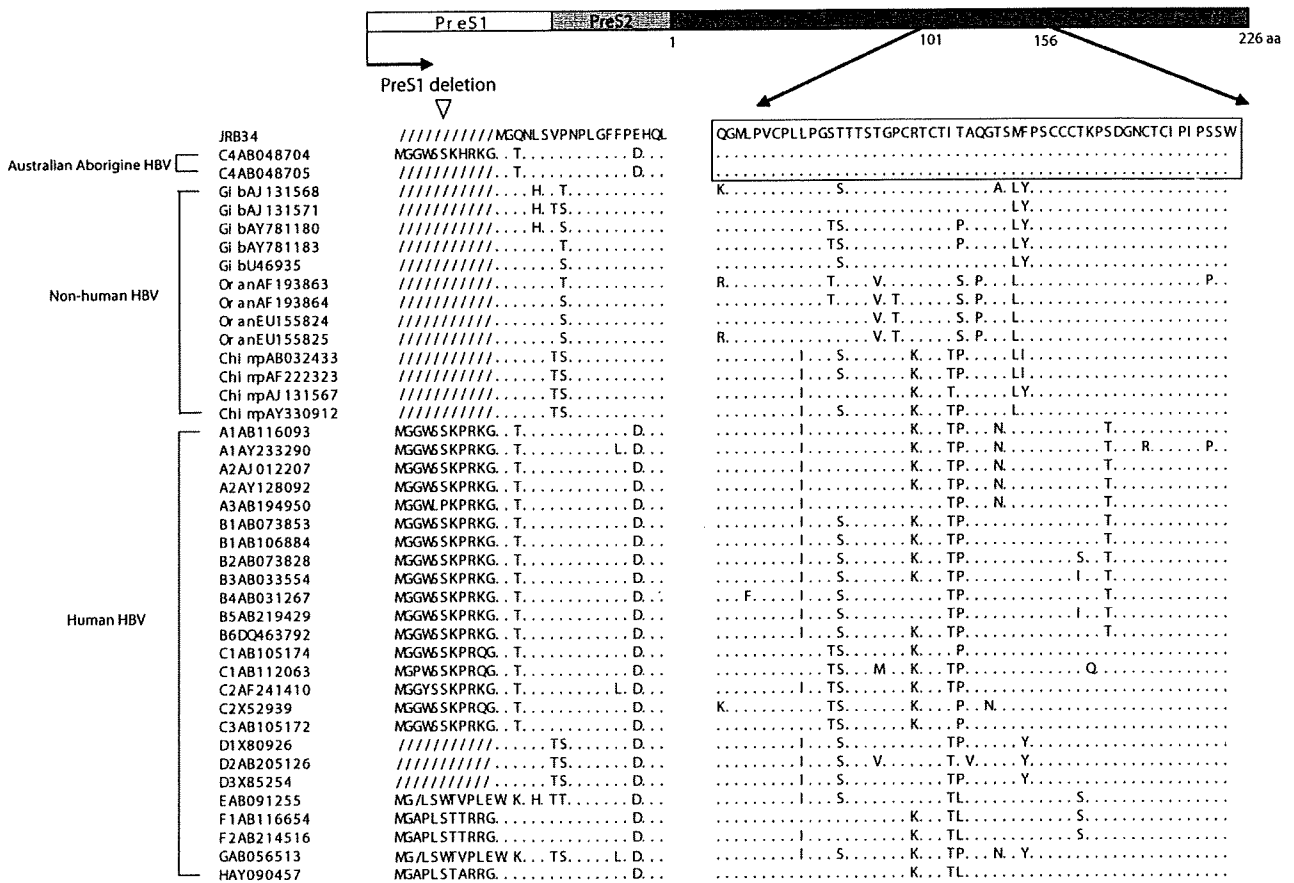


FIG. 5. Comparison of amino acid sequences of the preS/S gene among HBV isolates of various genotypes. The sequence of the HBV/J isolate (JRB34) is indicated at the top. Dots represent amino acids shared by JRB34, and a dash indicates the deletion of an amino acid. The sequence from positions 101 to 156 forming loops, bearing the common antigenic determinants of HBsAg, is boxed.

genes) and genotype C (in the core gene). However, no significant evidence of recombination between these two ape and human genotypes was revealed by the used methods. Homology scan carried out by SimPlot using the same set of reference sequences gave concordant results.

Phylogenetic analyses of the four open reading frames. Phylogenetic relationship between the JRB34 strain and other genotypes was further analyzed in four open reading frames. In the small S gene, subgenotype C4 recovered from Australian aborigines (43) changed its phylogenetic topology from the branch of human genotypes to a branch intermediate between orangutan and gibbon strains (Fig. 3A). Remarkably, genotype J and C4 strains joined together to create a clade between orangutan and gibbon strains. In contrast, genotype J clustered with human genotypes in the phylogenetic analysis of the C gene and was closely related to genotype C; it took a position outside genotype I strains, however (Fig. 3B). Genotype J was closer to gibbon and orangutan genotypes in the phylogenetic trees constructed on P and large S genes (data not shown), demonstrating its topology similar to that in the analysis of the entire genome (Fig. 1).

Amino acid sequence of the HBV/J isolate. The amino acid sequence of HBV/J was compared against those of other genotypes over three different areas of the genome. The amino

acid sequence in the preC gene and arginine-rich domain in the carboxy-terminal sequence in the C gene were well conserved by genotype J (Fig. 4). In the preS1 region, genotype J had a deletion of 11 aa as gibbon and chimpanzee genotypes (Fig. 5). This deletion was shared by one of the two HBV/C4 isolates from Australian aborigines, as well as all HBV/D isolates. Amino acid sequence in the S gene of genotype J was the same as those of aborigine isolates of subgenotype C4; they would share antigenic epitopes of HBsAg. Amino acids at codons 122 and 160 were arginine (with G as nt 365) and lysine (with G as nt 479), respectively, which was consistent with subtype *ayw* of HBsAg from this patient (27).

Five domains (A to E) of DNA polymerase/reverse transcriptase in the P gene were preserved well in HBV/J, and it did not have mutations in the Tyr-Met-Asp-Asp motif in the domain C that determines the sensitivity to lamivudine (data not shown). HBV/J possessed A1762T/G1764A double mutations in the core promoter and G1896A stop codon mutation in the preC region, which was compatible with an HBeAg-minus phenotype of HBV recovered from the patient positive for anti-HBe.

Infection with HBV/J in chimeric mice with the liver repopulated for human hepatocytes. Two chimeric mice that had been transplanted with human hepatocytes were inoculated with 10⁴ HBV DNA copies of genotype J. In both mice, HBV

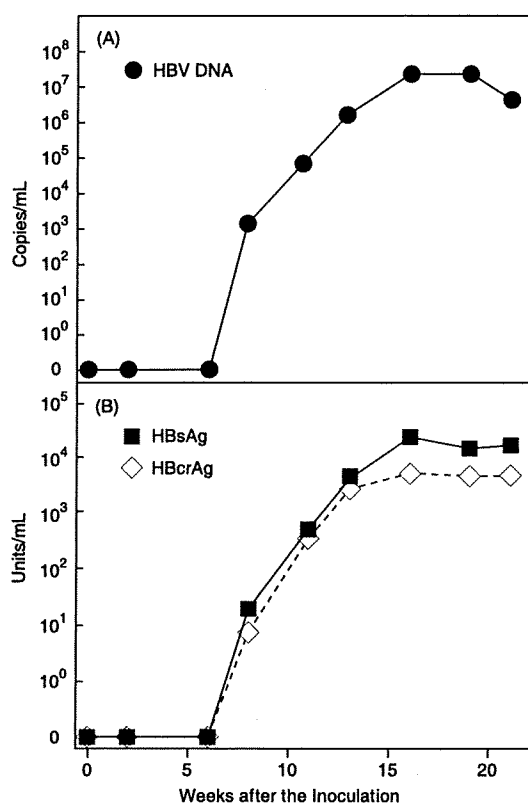


FIG. 6. Markers of HBV infection in two chimeric mice inoculated with the HBV/J isolate (JRB34). The levels of HBV DNA are illustrated in panel A, and those of HBsAg and HBcAg are illustrated in panel B. Values represent the means for two mice.

DNA in a high titer (10^5 copies/ml) appeared in the circulation at week 7, plateaued at high levels (10^6 to 10^8 copies/ml), and stayed detectable until 22 weeks of observation after the inoculation (Fig. 6A). HBsAg and HBcAg became detectable at week 7 and kept increasing in concentrations until week 15 when they reached a plateau at high levels (Fig. 6B). HBV strains recovered from mice at the last day of follow-up were identical in the complete genome sequence to the JRB34 strain used for inoculation.

The liver from chimeric mice infected with HBV/J was stained for HBcAg by immunofluorescence (Fig. 7A). The staining for HBcAg was confined to areas where mouse liver had been replaced for human hepatocytes, and the same areas were stained for human albumin (Fig. 7B). Colocalization of HBcAg and human hepatocytes was demonstrated by double staining for HBcAg and human albumin (Fig. 7C). Finally, expression and replication of the JRB34 strain were confirmed by successful detection of cccDNA and HBV RNA in the liver tissue from both sacrificed mice (see Fig. S2A and B in the supplemental material).

DISCUSSION

An HBV isolate (JRB34) was recovered from a male, 88-year-old Japanese patient with HCC and sequenced over the entire genome. In the full-genome sequence, the JRB34 strain

had 10.9 to 15.7% divergence from 1,440 HBV strains retrieved from the DDBJ/EMBL/GenBank. The divergence exceeds 8% that has been defined originally for distinguishing between four genotypes (A to D) (29) and later for an additional four genotypes (E to H) (3, 26, 42). Phylogenetically, the sequence of JRB34 was closer to ape than human HBV genotypes. No significant evidence of recombination with eight known human and four ape genotypes was revealed by the GroupScanning analysis (40) and phylogenetic analyses. These lines of evidence have qualified the JRB34 strain to represent a possible new HBV genotype. To further confirm the epidemiological significance of this strain, capable of establishing new infections, two chimeric mice were each inoculated with 10^4 copies of JRB34 HBV DNA. They both were successfully infected with sharp increases in HBV DNA and HBsAg in serum several weeks after the inoculation. Replication in the chimeric mice was also confirmed by detection of cccDNA and HBV RNA in their liver tissues.

Recently, an HBV isolate from Vietnam (VH24 [accession no. AB231908]) was reported as a ninth human genotype (I) (12). However, VH24 differed by only $7.0\% \pm 0.4\%$ from HBV isolates of genotype C and possessed complex recombination with genotypes A and G in three genomic areas. A number of sporadic HBV isolates have been reported to date that contain recombination between human genotypes (4, 24, 40), as well as between human and ape genotypes (21). Only a few recombinant variants, however, became widely spread in human populations, developing their own specific distributions and epidemiologies. This is particularly demonstrated for the B/C recombinant designated as a distinct subgenotype; Ba/B2-5 now accounts for the majority of genotype B strains in mainland Asia (44). Likewise, the C/D recombinant prevails in Tibet and northern China (50). To avoid assigning a new genotype for every newly discovered sporadic recombinant HBV variant, evidence of intergenotypic recombination should be carefully eliminated (14). However, in some cases, designation of a new genotype is proposed by a potential epidemiological significance of a novel genetic variant. Recently, a study carried out in Laos described a number of strains closely related phylogenetically with the Vietnamese genotype I strains, thereby suggesting their epidemiological significance (31). The JRB34 strain documented in the present study was genetically and phylogenetically distinct from any previously published strains, including those of genotype I from Vietnam and Laos. To avoid possible misconceptions in the future, the strain is provisionally designated genotype J.

HBV of distinct genotypes can infect great apes in the wild, including chimpanzee, gorilla, orangutan and gibbons (9, 20, 37, 51). HBV genotypes of chimpanzee and gorilla, as well as those of orangutan and gibbon, cocluster in agreement with their geographical distribution in Africa and Southeast Asia, respectively (41). Genotype J represented by the JRB34 strain clustered with gibbon/orangutan genotypes. In a phylogenetic analysis of the S region/gene sequence, JRB34 belonged to a nonhuman HBV group but was closely related to an HBV isolate of subgenotype C4 (AB048704) recovered from an Australian aborigine; C4 is most divergent from other subgenotypes of genotype C (43). In the phylogenetic analysis of the C gene, however, JRB34 clustered with human genotypes and closely related to genotype C, including C4, and was positioned